AN INVESTIGATION OF THE EFFECTS OF AIR TEMPERATURE ON BENZENE SPRAY VAPORIZATION

A Thesis submitted to the
Faculty of the Graduate School of the
University of Minnesota

by

Joseph R. Hawvermale
LT, U.S.Navy

In Partial Fullfillment of the Requirements
for the Degree of
Master of Science in Aeronautical Engineering

May 1957

ACKNOWLEDGMENTS

I wish to express appreciation to Professor Thomas E. Murphy for his guidance and encouragement, to LT John A. Hess for his assistance, and to William J. Alden for his assistance in construction of the apparatus.

This project was sponsored by the United States Navy, through the United States Naval Post-Graduate School program, and used the combined facilities of the Aeronautical and Mechanical Engineering Departments of the University of Minnesota.

SUMMARY

It was the purpose of this investigation to determine the effect of changing inlet air temperature on the vaporization of benzene fuel sprays under conditions similar to that encountered in jet engine combustors. This was done by photographing the fuel spray and, by measurement of the fuel droplets, determining the mass of fuel present in the spray.

It was found that air temperature has its greatest effect at short distances from the fuel injector and that this effect diminished as the distance was increased. An empirical formula was derived that correlated the percent of fuel remaining unevaporated with inlet air temperature, distance from the fuel injector, and the boiling point of the fuel. This formula is:

$$M^{*} = \frac{K}{\left[\frac{Ta}{3300}\right]^{\frac{BP}{257}} \left[\frac{d}{9.1}\right]^{1.73}}$$

where K is a factor dependent upon the fuel being considered. Correlation was obtained between benzene, isooctane and JP-5 jet fuel.

AN INVESTIGATION OF THE EFFECTS OF AIR TEMPERATURE ON BENZENE SPRAY VAPORIZATION

INTRODUCTION

One of the primary design considerations in the development of a jet engine is the ignition delay of the fuel. This ignition delay is the time interval between fuel injection and fuel burning. Since the fuel cannot burn until it has vaporized and mixed with the air to form a combustible mixture, the ignition delay is influenced greatly by the vaporization rate of the fuel. Anything that can be done to hasten the vaporization of the fuel will reduce this delay. With a smaller delay time, the combustor can be made shorter and more compact, with appreciable saving of space and weight in the engine.

The vaporization rate of a single drop of volatile fuel in still air is dependent upon three primary factors:[1].

1. The condition of the ambient air, measured by its pressure and temperature.
2. The fuel used and its properties, namely vapor

pressure, diffusion coefficient and thermal conductivity.

3. The initial conditions of the drop, that is, fuel temperature and drop size.

If the air is now given velocity relative to this single drop, the relative velocity between the fuel drop and air will influence the vaporization rate.[2].

Now if the single fuel drop becomes a fuel spray, the spray density will effect the vaporization rate of the fuel in the air. This effect may be visualized by imagining one fuel droplet traveling immediately behind another. The first droplet's vaporization would be determined by the single drop factors outlined above, but the vaporization of the second droplet must be slowed because of the fuel vapor already in its path. This interference effect of one drop upon another appreciably increases the difficulty in making a rational derivation of spray vaporization rates.

Fuel injected through a nozzle into a combustor passes through the following stages. The fuel leaves the nozzle orifice as a ligament or sheet. The turbulence of the primary air flow and shearing stresses within the fluid ligament break down the ligament into different size droplets. Appreciable heat transfer from the air present in the combustor to the fuel occurs only after the ligament has broken up into droplets. This is due to the appreciable increase of surface area of the fuel that is exposed to the air.[2]. The heat

transfer mechanims is mostly conduction and convection. The radiant energy transfer from the flame front and combustor walls is not significant in present day combustors.[3].

As heat transfer takes place between the air and fuel drops, the droplets heat up and at the same time, lose part of their mass by vaporization and diffusion into the air, with both heat and mass transfer being markedly affected by spray droplet size and velocity relative to the air. The smaller the drop size, the greater surface area of the spray, hence the greater heat and mass transfer.[2]. Also, the higher the relative velocity of the spray, the greater the heat and mass transfer, since the blanket of air and vapor surrounding each drop is being stripped away faster.

The droplets are also slowed down (or speeded up) relative to the air by aerodynamic drag forces. The smaller droplets lose their mass faster and evaporate faster than the larger droplets. Thus, a cloud of vapor due to the smaller droplets is rapidly formed and moves along with the air. The mass of vapor produced by the larger droplets is added to this vapor cloud. Somewhere in the combustor, a combustible mixture of air and fuel vapor is formed and is ready for ignition at that point.[2].

Some work has been done on vaporization rates of single drops. Ingebo obtained vaporization rates of pure liquid drops by injecting the liquid into a cork

sphere in a moving airstream and measuring the mass flow of liquid necessary to keep the cork sphere wetted.[4]. He continued his work by next determining the effect of pressure on the vaporization rates of single drops.[5].

El-Wakil has made a theoretical investigation of the unsteady state portion of single drop vaporization[2]. and has calculated temperature and mass histories of vaporizing drops.[1].

One method of obtaining spray data is by photographic means. York and Stubbs outlined an expermental method for determining the size distribution and velocities of drops in a water spray.[6]. Ingebo used a modification of this method in his study of spray vaporization rates, obtaining photomicrographs of sprays with a droplet camera developed at the NACA Lewis Laboratories.[7].

It is the intention of this project to measure the effect of temperature on benzene spray vaporization. Benzene was selected as the fuel for availability and economic reasons and for the fact that it is a pure hydrocarbon. Table I lists the properties of Benzene. The fuel is sprayed into a wind tunnel air stream heated to various temperatures and the spray photographed. From the photographs, the mass of fuel evaporated is determined. The following parameters are held constant; fuel temperature, pressure of injection, nozzle orifice,

air velocity and air pressure. Air temperature is varied and the spray photographed at various distances from the nozzle.

EQUIPMENT

The wind tunnel used is, basically, the one described in Ref. (8) with various improvements and modifications incorporated. Some of these modifications are described in Ref. (9). Additional alterations were made, the main one being that of suspending the tunnel in a vertical position. Fig. 1 is a schematic of the wind tunnel in its final configuration and Fig. 2 is a composite photograph of the tunnel.

The tunnel walls are one-eighth inch steel, welded together and reinforced with angle iron strips. The settling chamber and the nozzle section are insulated with a one inch fibreglass blanket covered by three-quarters inch magnesia cement and finished by a canvas wrapping.

Air is drawn through the tunnel by means of a vacumn created at the air inlet side to a centrifugal compressor. The compressor is driven by a 165 horsepower Lycoming tank engine with a gear ratio of 7.48:1. Fig. 3 is a photograph of the tank engine and Fig. 4 of the compressor. The engine is controlled by the throttle adjustment at a remote control station panel.

The air flow path is through an air inlet valve

at the top of the tunnel, thence through a heater section equipped with twelve chromalax 230 volt, 2350 watt, fin strip electric heater. These heaters are controlled by a switch board adjacent to the tunnel and two variac units. Fig. 5 and Fig. 6 are diagrams of the heater location and wiring diagram.

From the heater section the air passes through the settling chamber which is equipped with three screens to damp large scale turbulence. The air is then accelerated through the nozzle section into the test section.

The air is drawn out of the test section through a 90° elbow equipped with an air bleed valve, thence into the ducting running to the compressor inlet. The diffuser and surge tank described in Ref. (8) and (9) was eliminated in modification.

The square test section has inside dimensions of four inches by four inches and a length of twenty inches. Two side walls are one-half inch thick pyrex glass for visual and photographic observation. Static pressure taps are drilled every inch along the center-line of the top wall of the test section, with large holes drilled in various locations for insertion of total pressure and temperature probes. See Fig. 7.

Fuel is injected into the air stream through a nozzle located on the test section axis at the test section entrance. A one-half inch pipe running axially

through the settling chamber and nozzle section serves as a mount for the fuel nozzle and a container for the one-eighth inch copper fuel tubing and coolant water.

The fuel system consists of a five gallon fuel tank that is pressurized from a carbon dioxide gas cylinder. See Fig. 8. The fuel tank is immersed in a water jacket and is maintained at water tap temperature. Two separate filters are installed in the fuel lines, one of which is a steel mesh hydraulic fluid filter, the other, an automotive engine oil cloth filter. The fuel line is equipped with a pressure gage and a control valve.

A fuel nozzle delivering a spray that was flat in one direction was required in order to eliminate wetting of the glass side walls of the test section. Wetting of these walls would prevent the taking of photographs along the length of the test section. Considerable difficulty was encountered in manufacturing such a nozzle with the required low delivery rate, however one nozzle was finally made that delivered .835 lbs. of benzene per minute at 80 p.s.i. pressure with a spray angle of twenty degrees in one direction. This nozzle is mounted in the tunnel and oriented so that the flat spray sheet is parallel to the glass side walls of the test section.

The camera used to photograph the spray is a 4 x 5 Speed Graphic with a Kodak Ektar f:4.5 lens.

A Tiffen +3 close up lens is mounted on the camera for more magnification in the photographs. The camera is mounted on an adjustable tripod equipped with an elevating rack so that the camera can be raised or lowered axially along the length of the test section. The film used was Kodak Royal Pan with a tungsten exposure index of 160. The negatives were developed with FR x-500 developer and printed on high contrast paper. See Fig. 9 for camera and light mounting positions.

The first attempt to photograph the spray was made using a carbon arc lamp and a plano-convex lens to concentrate the light. A mirror mounted on an electric motor was used as a chopper in the light beam to reflect the light into the test section. However, the electric motor could not be run fast enough to stop the spray drop images on the film and this apparatus was abandoned. Fig. 10 is an example photograph obtained with this apparatus.

The light source finally used was a GE AH-6 mercury arc lamp powered by a thyratron electronic circuit designed and built by the Rosemount Research Center of the University of Minnesota. This light source yielded the excellent photograph of Fig. 11 which shows a conical spray nozzle delivering benzene. The lamp has a flash duration of six microseconds and a power of approximately 125 watt-seconds. The light flash is controlled by the trigger switch in the circuit. See Fig. 12 for the wiring diagram of the power supply.

Several light positions and camera settings were tried with the best photographs resulting from a camera setting of f:16 and the light placed at a sixty degree angle from the camera axis on the opposite side of the test section as shown in Fig. 9. All photographs of test runs were taken with this set up. Due to the limited space available, the light had to be moved to the upper alternate position as the camera was lowered. However, this caused no apparent change in the quality of the photographs.

Instrumentation for the tunnel was as follows:

A. Temperature measurements.

Three iron-constantin thermocouples were used to measure the necessary temperatures. These thermocouples were wired through a switchboard to a direct reading Leeds and Northrup potentiometer. The thermocouple locations were:

1. The center of the test section to provide inlet air temperature before spraying of fuel began. This thermocouple was inserted into tap number four (see Fig. 7) and was mounted inside a brass shield attached to a small diameter tube. The tube ran through a packing gland inserted in the test section tap so that the thermocouple could be withdrawn from the camera field of view before a photograph was taken at that station.

2. The cooling water outlet to provide cooling water exit temperature.

3. The duct to the compressor inlet to read compressor inlet air temperature.

The temperature of the fuel tank water bath was read by means of a standard mercury thermometer.

B. Pressure Measurements.

Three pressures were recorded for each test run. These were:

1. Test section static pressure; a standard mercury manometer was connected to a static pressure tap at station X = 1 inch of the test section.

2. Test section dynamic pressure; an inclined tube alcohol manometer was used, one side of which was connected to a total pressure probe inserted into test section tap number one (see Fig. 7) and the other side connected to a static pressure tap at station X = 0 of the test section.

3. Fuel pressure was measured by a standard Bourdon tube pressure gage inserted in the fuel line near the fuel control valve.

PROCEDURE

The first modification made to the wind tunnel was to suspend the tunnel vertically from the overhead. Temperature profiles were then measured to see if the large temperature gradients reported in Ref. (9) had been corrected. These profiles are shown in Fig. 13,

showing a still unsatisfactory, but symmetrical, temperature gradient. The tunnel was then insulated with magnesia cement and canvas, and temperature profiles again measured at four different temperature levels. These profiles are shown in Fig. 14 and indicate an acceptably flat gradient.

Velocity profiles were then measured and are plotted in Fig. 15. These measurements indicate a good velocity distribution throughout the test section and exhibit the characteristic shape of turbulent air flow.

The tunnel operating variables were static pressure, dynamic pressure, and temperature. These variables determined the air density and velocity. Nomographs were calculated and plotted so that air velocity could be quickly determined.

It was desired to simulate as closely as possible the conditions present in the combustion chamber of a jet engine, while varying the inlet air temperature. Accordingly, the inlet air velocity was set at 50 ft. per second which is a representative value, for combustors. (Ref. 10). This velocity was close to the minimum velocity at which the tunnel could be operated safely as the electric heaters require a cooling air flow of 50 ft. per second to prevent damage to the heaters.

Tunnel static pressure could be varied from 25 in. of mercury to 29 in., depending upon atmospheric pressure. The test pressure of 27 in. was selected as

mid range.

Tunnel temperature was varied from ambient air temperature to about 410° F depending upon air velocity.

Prior to starting the prime mover, the fuel tank was filled, capped, and pressurized to 80 p.s.i. The water jacket was filled with tap water and the water jacket temperature recorded. The prime mover fuel tank was filled to prevent engine stoppage due to fuel starvation while the heaters were on. The barometric pressure was read from a standard mercury barometer and recorded, and the manometers were zeroed.

The prime mover was then started and the desired number of heaters turned on. While the tunnel was coming up to temperature, the thermocouples and potentiometer were checked for proper operation. The camera was set up and focused on a .020 inch wire inserted through one of the static pressure taps. The camera was then elevated to station 5 and loaded with film.

By manipulation of the air inlet valve, the air bleed valve and the prime mover speed, the desired static pressure and dynamic pressure were set in the tunnel. The dynamic pressure was determined from the nomograph for the desired velocity and the temperature in the tunnel. When the operating conditions were reached, the mercury arc lamp power supply was turned on. During the three minute warm up period of the

power supply, adjustments of the camera, light, and tunnel operating variables were rechecked and recorded. The water exit temperature was recorded and compressor inlet temperature checked to see if it was within limits. If the compressor inlet temperature was too high, the water quench spray in the compressor ducting was turned on.

When the mercury arc lamp was ready for operation, the room lights were turned out and the doors closed. The fuel spray was then turned on and the fuel pressure adjusted to 80 p.s.i.

The camera shutter was then cocked, opened, the mercury lamp flashed, and the shutter closed. The fuel spray was turned off while the camera was lowered to the next station and the lamp adjusted. The process was repeated until photographs at four stations were obtained for each test temperature. These stations were X = 5, 10, 13.75 and 17.5 inches from the nozzle. These distances were determined by measuring and marking the rack of the camera tripod.

At the completion of each test temperature run, the lights were turned on, the room ventilated and the heaters adjusted for the next temperature. The camera was reset at station 5 and the focus checked again with the wire. When the tunnel temperature reached the next test point, the above procedure was repeated.

Tunnel shut down consisted of turning off the

heaters and running the compressor at high speed until the tunnel cooled sufficiently to prevent damage to the heaters. The prime mover was then stopped and the fuel system de-pressurized.

A photograph was taken of the .020 inch wire to provide a measure of magnification in the final enlargements and to establish a scale factor for drop size measurements.

The photographic plates were then processed and examined for quality before enlargement.

Table II lists the test conditions under which the photographs were made.

RESULTS

The ideal way to study the vaporization history of a spray would be to select a group of spray droplets as soon as they are formed and follow this group along the length of the test section. Since the photographic equipment was not available to do this, the best alternative was to select equivalent areas in the spray to study. The condition of constant velocity of the spray relative to the air dictated the selection of equal area lengths, at each of the four photographic stations along the test section. The selection of area widths was based upon the spreading of the spray across the test section due to the nozzle spray angle of 20°, the widest area being selected at a distance of 17.5 in.

from the nozzle and proportionately narrower areas selected as the distance from the nozzle decreased. Thus, the same number of drops should be included in each photograph at a given temperature, provided no evaporation took place.

From this consideration of the spray geometry and the enlarging equipment available, areas of the spray photographs were selected for enlargement as indicated in Fig. 16. Accordingly, these areas were outlined on the negatives in india ink and enlarged approximately five times. All photographs were enlarged the same amount and from measurements of the enlargement of the .020 inch wire, the total magnification factor of 1:10.75 was established. Figs. 17 thru 20 are enlarged photographs of the spray at station 10. With the enlarged prints available, the counting and measuring of the spray drops could be accomplished.

A sheet of plexiglass was ruled off in small rectangles to use as an overlay on the photographs. This overlay sub-divided the enlargements into small areas as an aid in counting and measuring the spray droplets.

A card was ruled with lines of varying width. The smallest line was .01 inch in width, which, with the enlarged scale, was equal to 23.6 microns actual measurement. Thus the smallest drops measured were 23.6 microns in diameter. From the .01 inch width line the measuring lines increased by a $\sqrt{2}$ progression,

approximately, to a width of .08 inches. Thus the largest drop measured was 189 microns in diameter. See Table III for drop size increments. By comparing each drop with the lines ruled on this card, the drop size was determined as each drop was counted. Since not all drops in the photographs were in focus, only the drops with sharp images were counted. A jewelers eye loupe of 7 X magnification was used to examine all drops that were borderline.

By photography, a direct determination of the amount of fuel present in the spray can be made. Since the volume of a fuel drop is determined by the cube of its diameter, the total volume of fuel present is represented by the product $\sum nD3$ where n is the number of drops in the spray and D is the diameter of each drop. Then by a conversion factor, $\sum nD^3$ can be changed to mass of fuel in pounds. See sample calculations. Therefore for each drop size increment in each photograph the product nD^3 was formed, then summed, yielding $\sum nD^3$ which is a measure of the volume of fuel remaining in the photograph. This data is summarized in Table IV.

In order to test the reproduceability of the drop-size count, one area was counted on two separate occasions, with a resulting variation of 17% in the final values of $\sum nD^3$ obtained. This variation was at a drop-size count level of $\sum nD^3 \approx 1800 \times 10^{-6}$. The error is admittedly large, but justifiable in view of the crude methods available for measuring drop sizes

and the large number of drops out of focus.

In forming the product nD^3 for each drop size, the upper value of the diameter increment was used rather than an arithmetic mean of the increment. In measuring the drop sizes with the ruled card, each drop was assigned a size according to the line which it nearest matched. Thus, drops both larger and smaller than a measuring line were assigned diameters of that line. The upper value of each increment then became an average value for each drop size with the exception of the first increment. An arithmetic mean should have been used for the first increment to be strictly correct, however, the upper value was used for consistency.

In Ref. (11) Bahr arrived at an empirical formula to express the degree of spray evaporation for iso-octane sprays. This formula is

$$\frac{N}{100-N} = 9.35\left[\frac{Ta}{1000}\right]^{4.4}\left[\frac{Va}{100}\right]^{.80} Pa^{-1.2} Pf^{.42} L^{.84}$$

where N is the percent of spray vaporization, Ta is the inlet air temperature in ^{o}R, Va is the inlet air velocity in feet per second, Pa is the inlet air pressure in inches of mercury absolute, Pf is the fuel injection pressure drop in pounds per square inch, and L is the axial distance from the fuel injector in inches. With all variables constant except inlet air temperature, the degree of spray vaporization is proportional to the air temperature to an exponent. Therefore on a log-log

plot, the mass of fuel remaining versus the inlet air temperature should plot as a straight line. Furthermore, for each axial distance from the injector, the lines should remain parallel but offset from each other by a constant, dependent upon the axial distance.

Accordingly, in Fig. 21, the uncorrected mass of fuel, $\sum nD^3$, is plotted against inlet air temperature at various distances from the nozzle. At a distance of five inches from the nozzle, the data points fall along a straight line very nicely. However, as the distance from the nozzle increases, the spread of the data points increases until at a distance of 17.5 inches from the nozzle, the agreement is very poor. This is due to the increased percentage of error that one large drop can introduce at the lower values of $\sum nD^3$. It is felt that this error cannot be reduced unless a more refined photographic technique is employed, namely, a greatly enlarged depth of field would permit more drops to be in focus and to be counted, thus eliminating the decisions to be made for each drop as to whether or not to count and measure that drop.

A straight line was drawn through the data points of Fig. 21 as a method of averaging the error present in the data. From these straight lines, average values of $\sum nD^3$ were read and recorded in Table IV. From the averaged values of $\sum nD^3$ the mass of fuel remaining was calculated and recorded in Table IV.

It was then necessary to determine the amount of fuel injected from the nozzle so that the percentage of fuel evaporated could be calculated. This was done by two different methods. The first method used was to plot the uncorrected $\sum nD^3$ values versus distance on a log-log graph using the various temperatures as parameters. These curves were extrapolated to a distance of three inches. See Fig. 22. At this distance, the values of $\sum nD^3$ were read, and plotted against temperature on a log-log graph. A straight line was drawn through the points to average them, and the averaged values replotted on the original graph. The curves were then extrapolated to 2.5 inches and the process repeated. The procedure was carried out in one half inch increments until a distance of one inch was reached. Here an average of the values was taken as the amount of fuel injected, with the assumption that no appreciable evaporation had occurred in the first inch of fuel travel from the nozzle. The amount of fuel injected was determined to be 1780×10^{-10} lbs. during the time interval covered by the photographs.

The second method used to determine the amount of fuel injected was by calculation based uponthe fuel delivery rate of the nozzle. See sample calculations. From these calculations, the amount of fuel injected was determined to be 2485×10^{-10} lbs.

The extrapolated value of 1780×10^{-10} lbs. was

used to calculate the percentage of fuel evaporated as it was felt that this value was the more accurate of the two. The calculated value was based upon several assumptions which were known to the approximations. The final graph of mass of fuel remaining versus distance from the nozzle is shown as Fig. 23 on a log-log plot. The percentage of fuel evaporated is plotted against air temperature in Fig. 24 and against distance from the nozzle in Fig. 25.

DISCUSSION

Since the objective of this investigation was to study the effect of varying air temperature on benzene sprays, it was desired to hold all other parameters constant. The fuel temperature, pressure of injection and fuel nozzle orifice were kept the same for each run. These parameters determine the amount of fuel injected into the test section. Therefore, the mass flow of fuel was constant, as was the initial velocity of the spray. The inlet air velocity was held constant so that the relative spray velocity did not change. The static air pressure was held constant at 27 inches of mercury. Since the air temperature varied, the air density and air mass flow varied. This caused the fuel-air ratio to vary, so that two parameters enter into the data presented; the varying fuel air ratio

and the varying inlet air temperature. With the equipment available, it was impossible to vary the air temperature alone, while holding all other parameters constant.

It was hoped that, with the flat spray nozzle, all drops in the spray would be in focus. However, this was not the case, as was apparent from the first photographs examined. By counting the number of drops in focus and then the total number of drops in the photograph for several plates, it was determined that the percentage of drops in focus averaged 38.5%. This was due to the extremely narrow photographic depth of field for the camera with the close up lens attached. Therefore, the mass of fuel as determined from the photographs represents only approximately 38.5% of the total fuel present. This factor was assumed to be constant and was taken into account when calculating the amount of fuel injected based upon the nozzle delivery rate. See sample calculations.

From a visual examination of the fuel delivery from the nozzle at low pressures, it could be seen that the fuel was concentrated towards the edges of the triangular spray as indicated in Fig. 26. The spray edges were solid streams of fuel while atomization was obtained only at the center of the spray. With increased fuel pressure, the whole spray became atomized but the fuel remained concentrated at the

spray edges. The spray density was not uniform, but had the distribution pattern indicated in Fig. 26. This is shown again in Fig. 27, which is a photograph of the spray edge at a distance from the nozzle of five inches.

A similar distribution pattern for conical sprays is reported in Ref. (12). From curves plotted in this reference, it was estimated that 75% of the fuel in the spray is concentrated in the outer edge of the spray. Therefore, the total mass of fuel delivered by the nozzle was reduced by 75% to allow for this non-uniform spray distribution.

Since the velocity of the drops in the spray could not be measured, it was calculated from the Bernoulli equation, $\frac{V_2^2}{2g} = \frac{V_1^2}{2g} \quad \frac{(P_1 - P_2)}{\gamma}$. The initial fuel velocity in the delivery pipe (V_1) was neglected as being small. Initial spray velocity was calculated to be 117.5 ft. per second for the fuel delivery pressure of 80 p.s.i. gage and was assumed to be constant throughout the length of the test section. It would have been desirable to have the initial fuel velocity the same as the inlet air velocity so that there would be no relative velocity between the spray droplets and the air. However, the high fuel delivery pressure was necessary to obtain good atomization from the nozzle.

These assumptions of constant spray velocity throughout the test section, a spray edge concentration

factor of 75%, and a constant percentage of drops in focus were used in the calculation of mass of fuel injected, and is the reason why the extrapolated value of 1780 x 10^{-10} lbs. was used in preference to the calculated value of 2485 x 10^{-10} lbs. The discrepancy in the two values is not considered to be serious, particularly when working with quantities of such small magnitude.

From the plot of percent fuel evaporated versus inlet air temperature (Fig. 24) it can be seen that the effect of increased air temperature was most pronounced at a distance of five inches from the nozzle. At this distance an increase of air temperature of 100%, from 150°F to 300°F, increased the percent vaporized by 33%. However, as the distance from the nozzle increased, the effect of increased air temperature diminished, until at 17.5 inches from the nozzle, their was very little effect. This was due to the very small droplets that evaporate in the first few inches of travel, creating a vapor cloud surrounding the remaining drops and slowing their evaporation. Then, too, the larger droplets are slower to evaporate because their heating up period is longer.

For the conditions under which this investigation was conducted, the axial distance from nozzle has a greater influence over fuel evaporation than does inlet air temperature as can be seen from Fig. 25. This figure is a cross plot of Fig. 24 and shows percent

of fuel evaporated plotted against distance from the nozzle using air temperature as the parameter. This greater influence of distance was due to the high volatility of the benzene, which allowed a very high degree of vaporization of the fuel droplets in the first few inches of travel. Also, the fuel delivery nozzle had a fine degree of atomization as can be seen in Fig. 28, a plot of typical drop size distribution. The greatest number of drops were of the smallest size range, from 0 to 50 microns.

It would have been of interest to investigate the fuel evaporation at points between the nozzle and station X = 5 inches from the nozzle. However, due to the amount of labor involved in counting and measuring the drops in each photograph and the shortage of time, this could not be done. An attempt was made to photograph the spray with ambient inlet air temperature of 84°F. Unfortunately, only two of these photographs were useable and were plotted only as substantiating evidence.

In order to correlate the results of this investigation with the work of others, data from Ref. (11) was plotted in Fig. 24. The data reported by Bahr was for iso-octane sprayed contra-stream to the air flow and measurements made at a station 10.4 inches from the nozzle. The higher evaporation rate of the benzene was due to the higher volatility of this fuel compared

to isooctane. Also, in Bahr's work, an air velocity of 193 ft per second was used, so that for equal distances from the nozzle, the isooctane had spent less time in the air stream than the benzene.

Again, in Fig. 25, data from Bahr was plotted, along with data reported by Ingebo in Ref.(7). In both instances the fuel was isooctane sprayed contra-stream with an inlet air temperature of 85 ^{o}F and an inlet air velocity of approximately 190 ft per second. Here too, the benzene exhibits a higher rate of evaporation due to the aforementioned volatility.

The percent of fuel remaining unevaporated was then plotted in Fig. 29 on a log-log plot. The slope for benzene evaporation was measured as .687 and was constant for each axial distance from the nozzle. Data for isooctane from Ref.(11) and data for JP-5 jet fuel from Ref.(13) are also plotted and have measured slopes of .982 and 1.4 respectively. Thus the evaporation of benzene is dependent upon some function of the air temperature, such as

$$M = kT_a^{-.687} .$$

One would not expect the rate of evaporation of all three fuels to be the same because of the difference in volatility and boiling points. For instance, benzene has a boiling point of 176 ^{o}F, isooctane is 243 ^{o}F, and JP-5 has an initial boiling point of 360 ^{o}F.

It was interesting to note that the slopes of these curves were in direct proportion to the boiling points of the fuels. Using this fact as a means of correlating the data, an empirical formula was derived for the percent mass of fuel remaining unevaporated. This formula is:

$$M^{*} = \frac{K}{\left[\frac{Ta}{3300}\right]^{\frac{BP}{257}} \left[\frac{d}{9.1}\right]^{1.73}}$$

where M^{*} is the calculated percent mass of fuel remaining unevaporated; Ta is the inlet air temperature in degrees Fahrenheit; BP is the fuel boiling point in degrees Fahrenheit; d is the distance from the nozzle in inches and K is a constant dependent upon the fuel used. The values of K were determined to be 1.70 for benzene; 2.94 for isooctane; and 4.05 for JP-5. See Appendix A for formula derivation.

Using the conditions under which the data was taken in Ref. (11) and (13), M was calculated for JP-5 and isooctane. M^{*} was calculated for benzene for the conditions of this investigation. The calculated percent of fuel remaining (M^{*}) was plotted against the measured percent of fuel remaining (M) in Fig. 30. This figure shows a very good one-to-one correlation between these two quantities for the three fuels considered.

Much work can be done to refine the techniques herein presented for the study of fuel sprays. It is felt that the equipment used is a very useful tool in

determining the effects of various parameters upon the evaporation of fuels. The use of photographic methods in spray studies is particularly attractive in that a direct measurement of fuel mass can be accomplished.

CONCLUSIONS AND RECOMMENDATIONS

It is concluded that:

1. The effect of air temperatures of finely atomized benzene sprays is most pronounced at short distances from the fuel nozzle.

2. The effect of an increased air temperature on benzene sprays diminishes as the distance from the nozzle is increased.

3. Benzene has a higher vaporization rate than isooctane or JP-5 because of its lower boiling point.

4. An empirical formula was derived that expresses the percent of fuel remaining unevaporated as a function of inlet air temperature, fuel boiling point, distance from the nozzle, and a factor, K, dependent upon the fuel being considered. This formula is:

$$M^{*} = \frac{K}{\left[\frac{Ta}{3300}\right]^{\frac{BP}{257}} \left[\frac{d}{9.1}\right]^{1.73}}$$

5. The values for K are: benzene, 1.70; isooctane, 2.94; and JP-5, 4.05 .

6. The formula gives good correlation for air

temperatures ranging from 150°F. to 600°F., distances from 5 to 17.5 inches from the nozzle and for the three fuels considered; benzene, isooctane and JP-5.

It is recommended that:

1. Photographic apparatus with a greater depth of field be used for furthur experiments.

2. A device to measure fuel droplet velocity be employed.

3. A variable area nozzle be used in order to isolate the fuel-air ratio as a parameter.

REFERENCES

1. El-Wakil, M.M., et al., "Experimental and Calculated Temperature and Mass Histories of Vaporizing Fuel Drops", National Advisory Committee for Aeronautics, Technical Note 3490, January 1956.
2. El-Wakil, M.M., et al., "A Theoretical Investigation of the Heating-Up Period of Injected Fuel Droplets Vaporizing in Air", National Advisory Committee for Aeronautics, Technical Note 3179, May 1954.
3. Berlad, A.L. and Hibbard, R.R., "The Effect of Radiant Energy on Vaporization and Combustion of Liquid Fuels", National Advisory Committee for Aeronautics, Research Memorandum E 52I09, November 1952.
4. Ingebo, R.D., "Vaporization Rates and Heat-Transfer Coefficients for Pure Liquid Drops", National Advisory Committee for Aeronautics, Technical Note 2368, July 1951.
5. Ingebo, R.D., "A Study of Pressure Effects on Vaporization Rates of Drops in Gas Streams", National Advisory Committee for Aeronautics, Technical Note 2850, January 1953.
6. York, J.L. and Stubbs, H.E., "Photographic Analysis of Sprays", American Society of Mechanical Engineers Transactions, Volume 74, 1952, pp. 1157-1162.
7. Ingebo, R.D., "Vaporization Rates and Drag Coefficients for Isooctane Sprays in Turbulent Air Streams", National Advisory Committee for Aeronautics, Technical Note 3265, October 1954.
8. Farnsworth, W.D., "The Design of a Wind Tunnel for Fuel Spray Vaporization Studies", A Master of Science Thesis submitted to the University of Minnesota, 1955.
9. Seligmiller, H.L., "An Investigation of the Distribution Pattern of Fuel Sprays Under Conditions of Interest in Jet Engines", A Master of Science Thesis submitted to the University of Minnesota, 1956.

10. Godsey, F.W. Jr. and Young, L.A., "Gas Turbines for Aircraft", First Edition, McGraw-Hill Book Company, Inc., New York, 1949.
11. Bahr, D.W., "Evaporation and Spreading of Isooctane Sprays in High-Velocity Air Streams", National Advisory Committee for Aeronautics, Research Memorandum E53I14, November 1953.
12. DeCorso, S.M. and Kemeny, G.A., "Effect of Ambient and Fuel Pressure on Nozzle Spray Angle", American Society of Mechanical Engineers Transactions, Volume 79, Number 3, pp. 607-615, April, 1957.
13. Foster, H.H. and Ingebo, R.D., "Evaporation of JP-5 Fuel Sprays in Air Streams", National Advisory Committee for Aeronautics, Research Memorandum E55K02, February 1956.

SYMBOLS and NOTATION

A - Area

BP - Fuel boiling point (^{o}F)

d - Distance from fuel nozzle (in)

D' - Acutal drop diameter (in)

D - Photograph drop diameter (in)

E - Percent fuel evaporated

g - Gravitational constant (32.2 ft/sec^{2})

h - Manometer reading (in. of alchol)

k - Empirical constant

m - Mass of fuel (lbs)

$\dot{m}$ - Mass flow (lbs/sec)

M - Percent fuel remaining, measured

M* - Percent fuel remaining, calculated

n - Number of drops

P - Static pressure

q - Dynamic pressure

R - Universal gas constant (24.22 in. Hg-$ft^{3}/slugs-^{o}R$)

T - Temperature (^{o}F)

t - Time (sec)

Vol- Volume

V - Velocity

γ - Specific weight (lbs/ft^3)

ρ - Density

μ - Microns

SUBSCRIPTS

a - Air

ave - Average

i - Initial

f - Fuel

T - Total

TABLE I

Properties of Benzene

Chemical Formula	C_6H_6
Molecular Weight	78.11
Hydrogen-Carbon Ratio	.0835
Boiling Point, ^{o}F	176
Specific Weight, lbs/ft^3	54.9
Specific Volume lbs/gal	7.31
Density, $Slugs/ft^3$	1.71
Stoichiometric Fuel/Air Ratio	.0754

TABLE II

TEST CONDITIONS

Test #	1	2	3	4	5
P_a in Hg	27	27	27	27	27
T_a ^{o}F	84	150	228	329	400
ρ_a slug/ft^3	.00205	.00183	.00162	.00141	.00129
V_a ft/sec	46.2	49.4	51.0	47.0	45.6
T_f ^{o}F	68	68	69	71	75
P_f lbs/in^2	80	80	80	80	80
F/A Ratio	.0411	.0432	.0472	.0586	.0658
d = 5 in	1	5	9	13	26
d = 10 in	-	6	10	14	27
d = 13.75 in	3	7	11-	15	28
d = 17.50 in	-	8	12	16	29

Photographic Plate Numbers

TABLE III

Drop Size Increments

Progression	1	$\sqrt{2}$	2	$2\sqrt{2}$	4	$4\sqrt{2}$	8
	1	1.41	2.00	2.83	4.00	5.66	8.00
Desired Dia.	.010	.014	.02	.028	.040	.056	.080
Actual Dia.	.010	.014	.020	.028	.040	.054	.080
$D^3 \times 10^{-6}$ (in^3)	1.00	2.74	8.00	21.9	64.0	145.	512.
D', Microns	23.6	33.0	47.2	66.0	94.5	127.5	189

Table IV

Data Summary

Plate	Ta	d	$\sum nD^3$	$\sum nD^3_{av}$	m	M	E
-	^{o}(F)	(in)	(in^3)	(in^3)	(lb)	(%)	(%)
-	-	-	$\times 10^6$	$\times 10^6$	$\times 10^{10}$	-	-
1	84	5	8000	7850	1052	59.1	40.9
3	84	13.75	1565	1380	185	10.4	89.6
5	150	5	5259	5220	700	39.3	60.7
6	150	10	1991	1860	249	14.0	86.0
7	150	13.75	849	920	124	7.0	93.0
8	150	17.50	449	565	74.5	4.2	95.8
9	228	5	4124	3910	524	29.4	70.6
10	228	10	1653	1400	187.5	10.5	89.5
11	228	13.75	662	680	91.2	5.1	94.6
12	228	17.50	504	420	56.3	3.2	96.8
13	329	5	2685	3050	408	22.9	77.1
14	329	10	949	1080	144.8	8.1	91.9
15	329	13.75	626	530	71.0	4.0	96.0
16	329	17.50	438	328	44.0	2.5	97.5
26	400	5	2650	2650	355	19.9	80.1
27	400	10	824	940	126	7.1	92.9
28	400	13.75	417	460	61.5	3.5	96.5
29	400	17.50	202	285	38.2	2.1	97.9

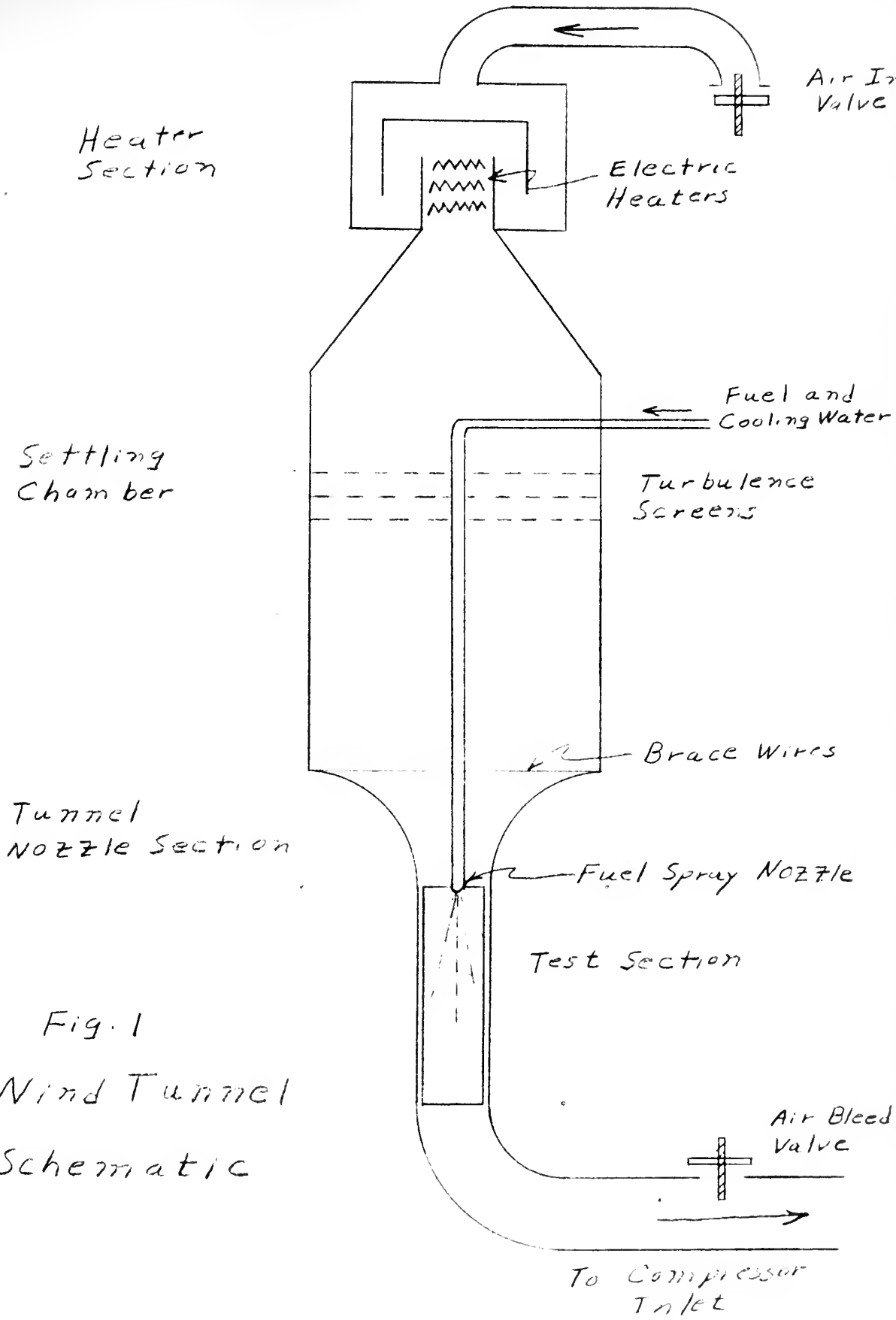

Fig. 1

Wind Tunnel Schematic

Fig. 2
Composite Photograph of
Wind Tunnel

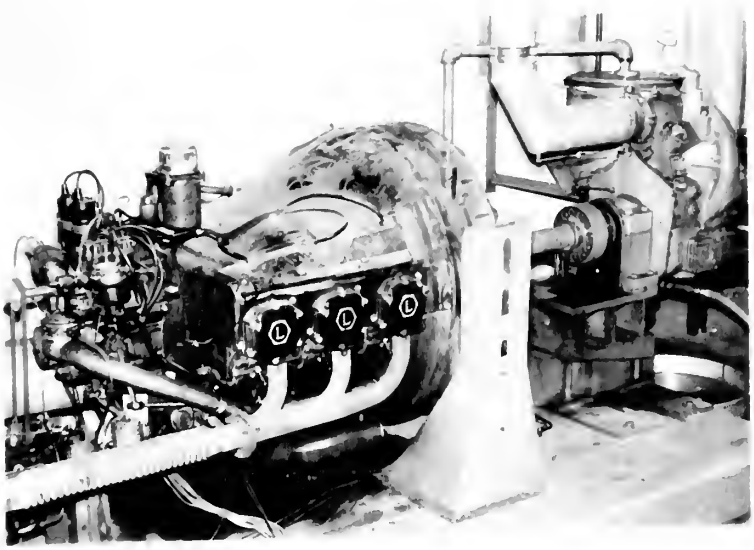

Fig. 3

The Prime Mover

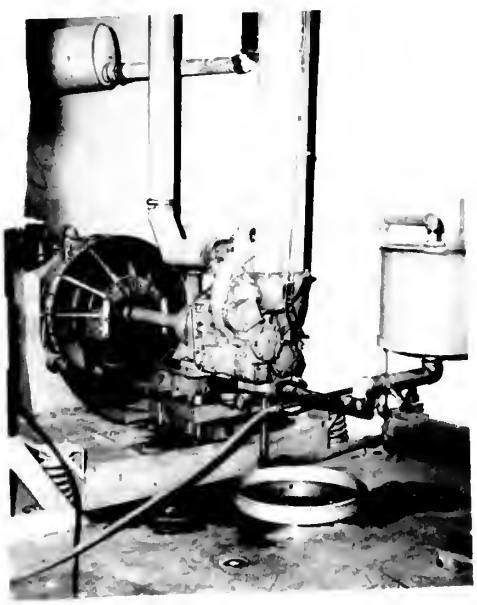

Fig. 4

The Compressor

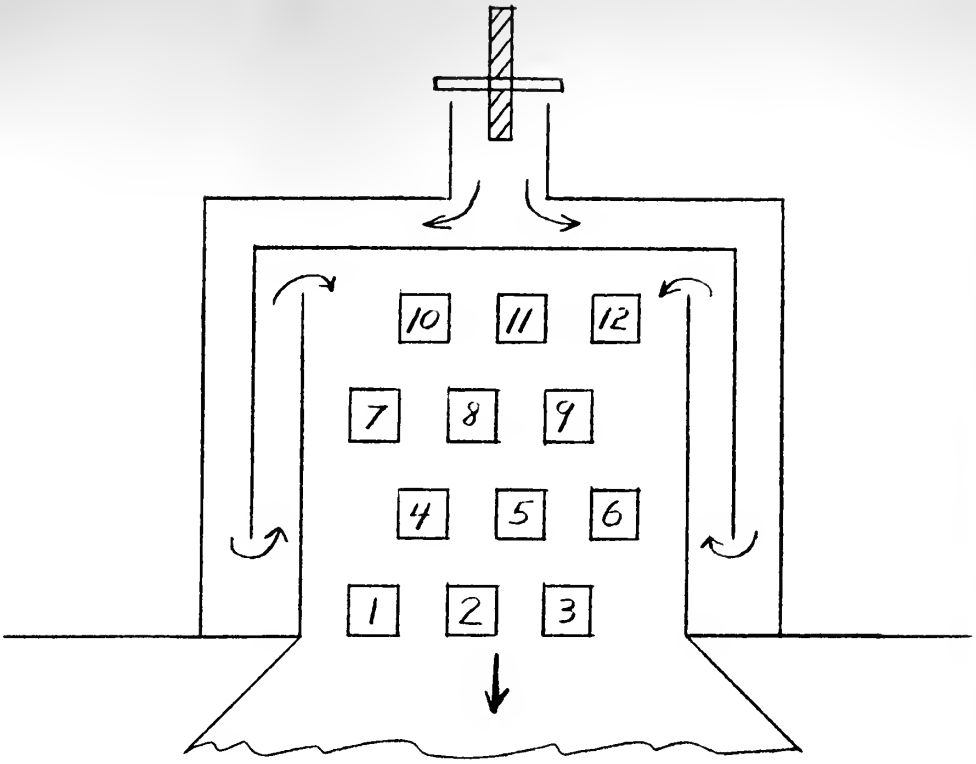

Fig. 5
Heater Installation

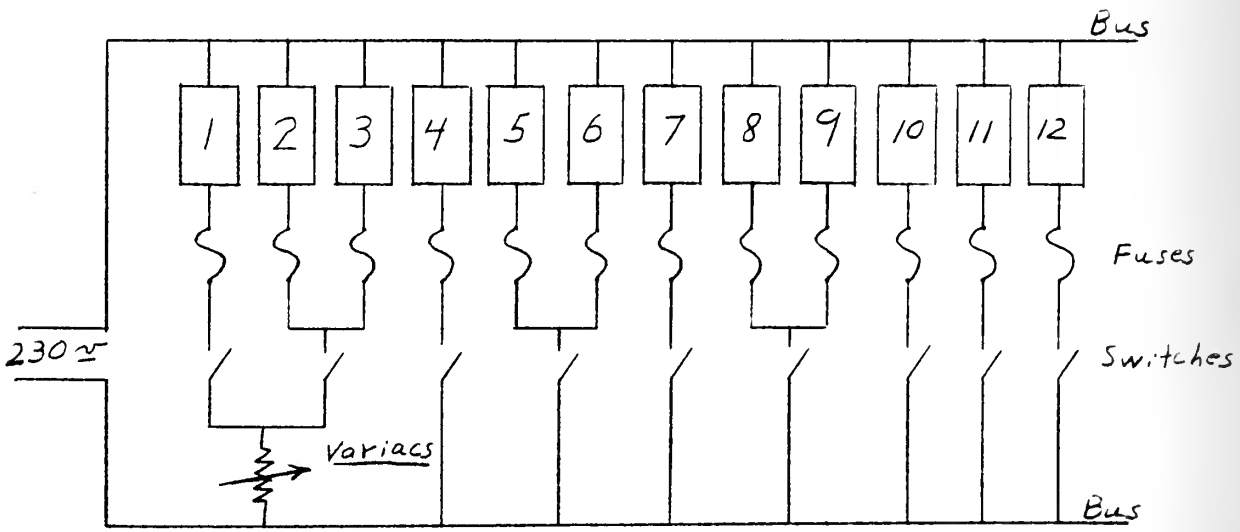

Fig. 6
Heater Wiring Diagram

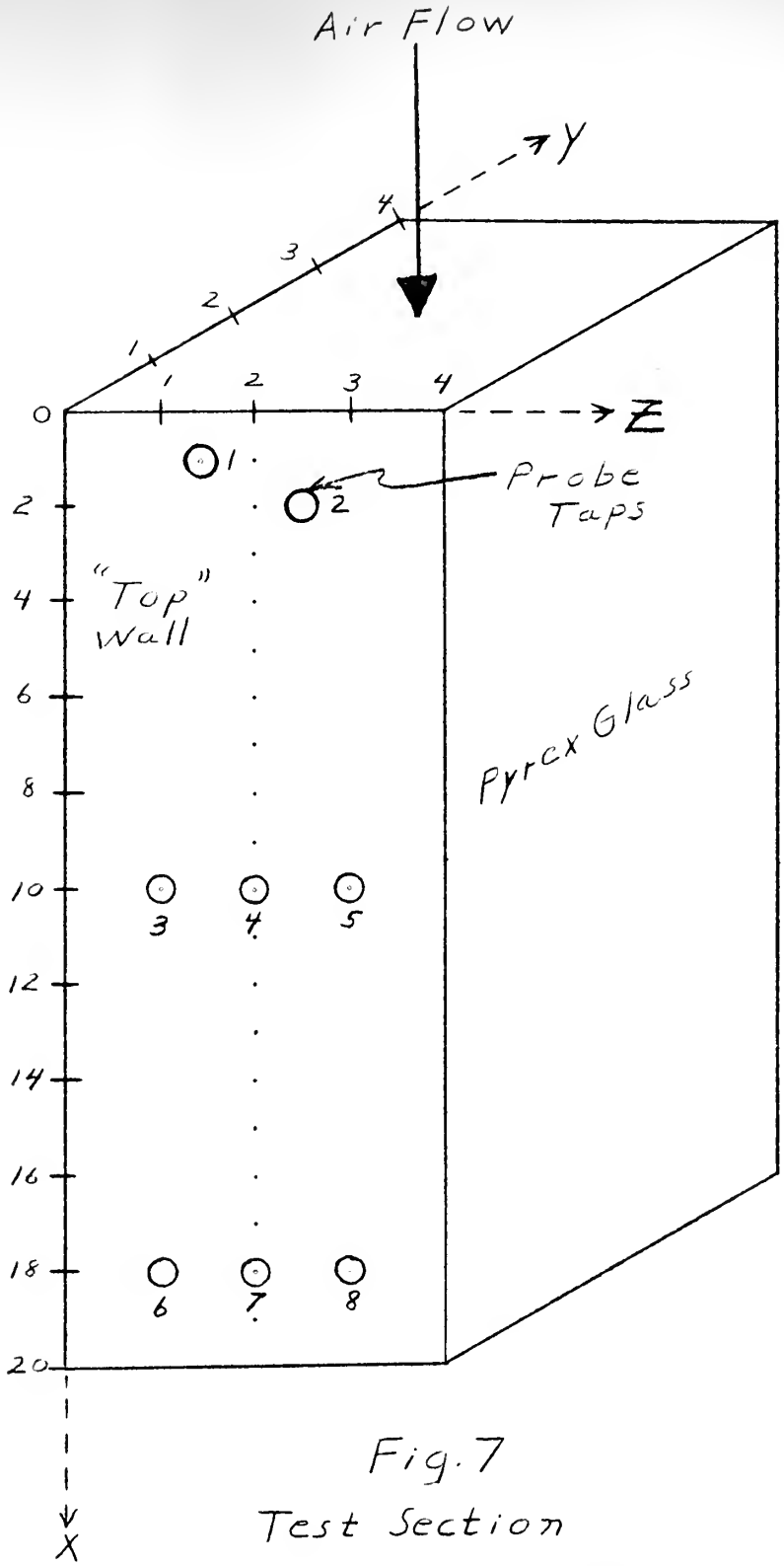

Fig. 7

Test Section Coordinate System and Tap Locations

Fig. 8

Fuel System showing CO_2 Tank
Water Bath, and Fuel Filter

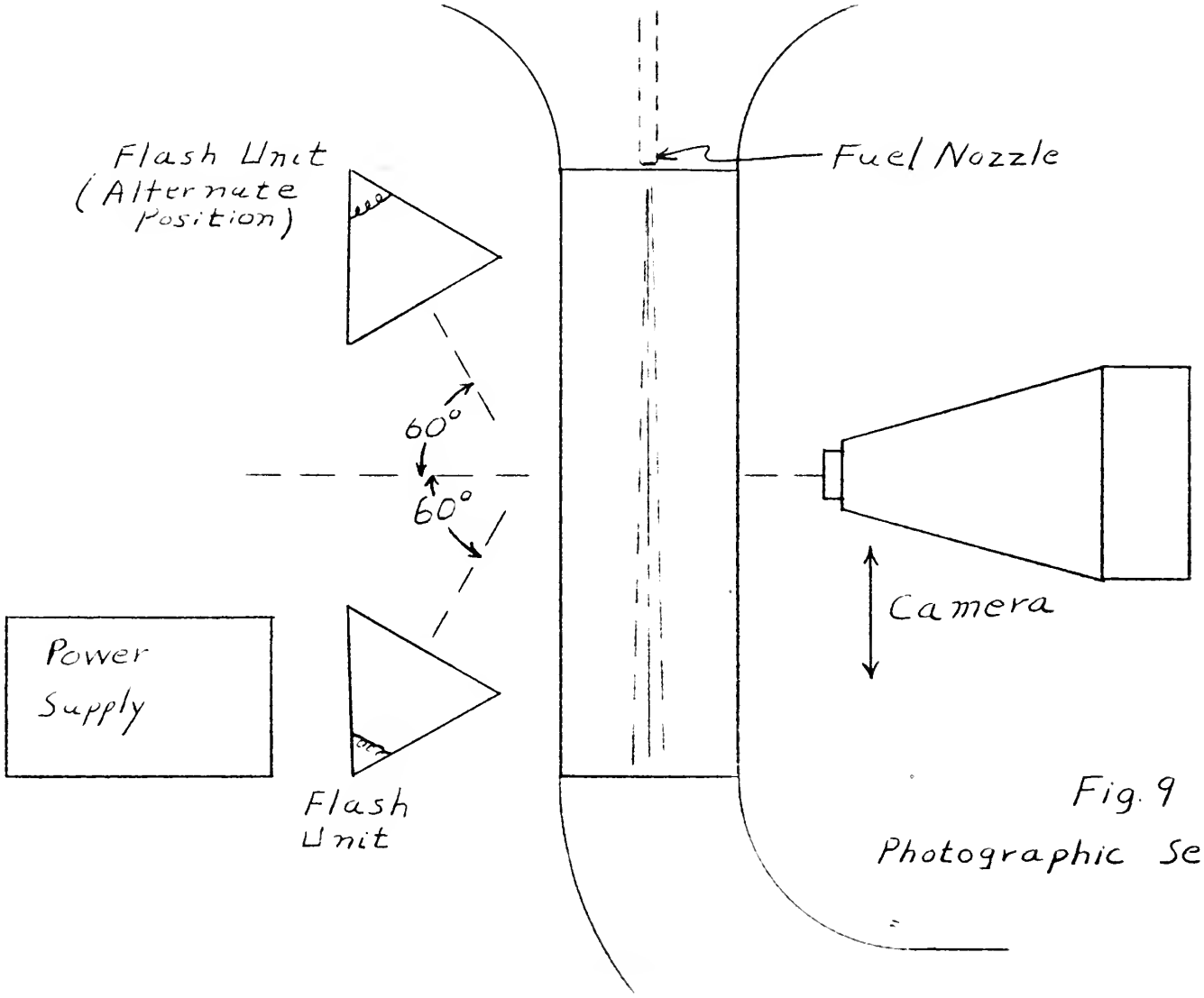

Fig. 9
Photographic Set-Up

Fig. 10
Spray Photograph Obtained
with Carbon Arc Lamp

Fig. 11
Spray Photograph Obtained
with Mercury Arc Lamp

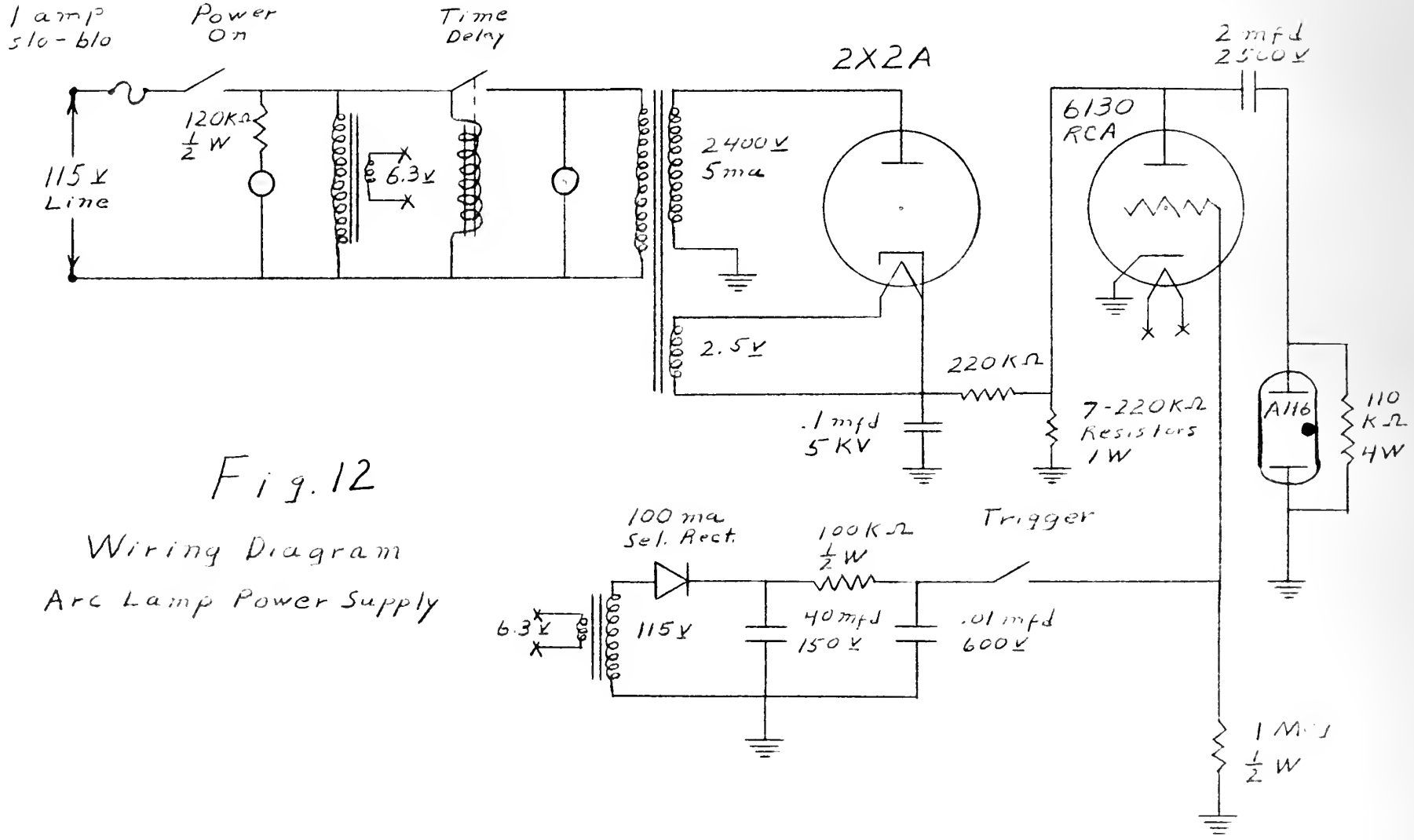

Fig. 12

Wiring Diagram

Arc Lamp Power Supply

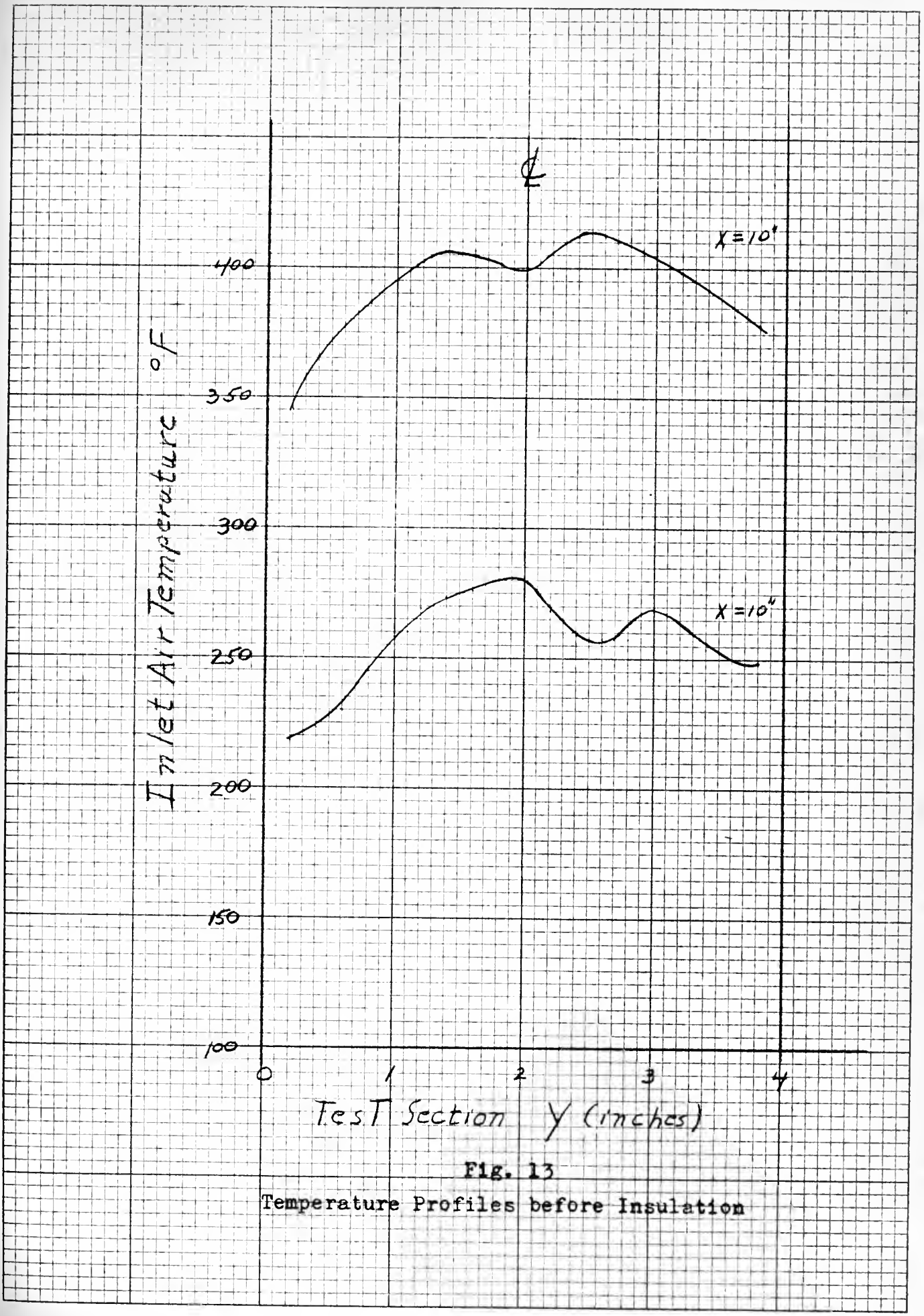

Fig. 13

Temperature Profiles before Insulation

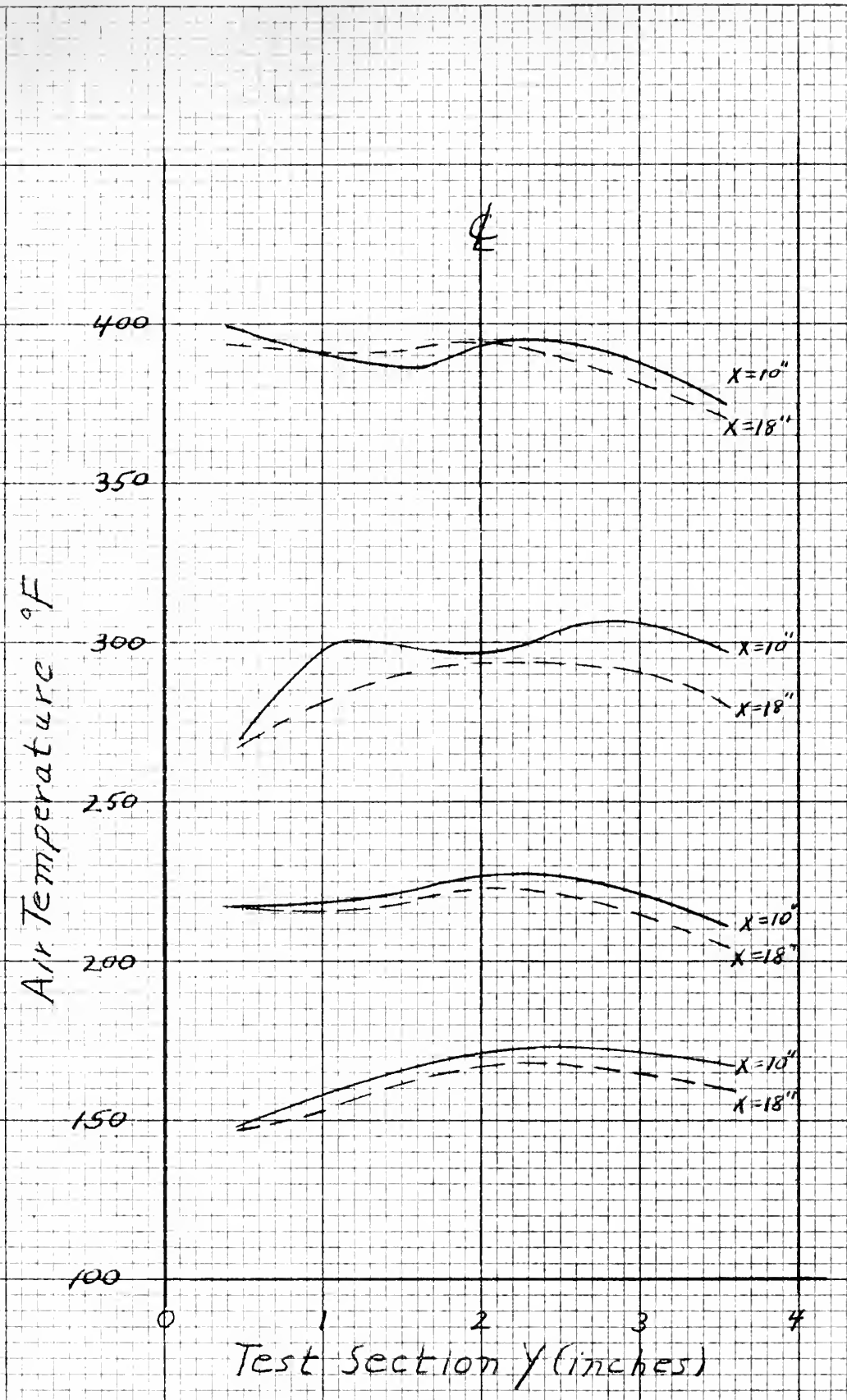

Fig. 14

Temperature Profiles after Insulation

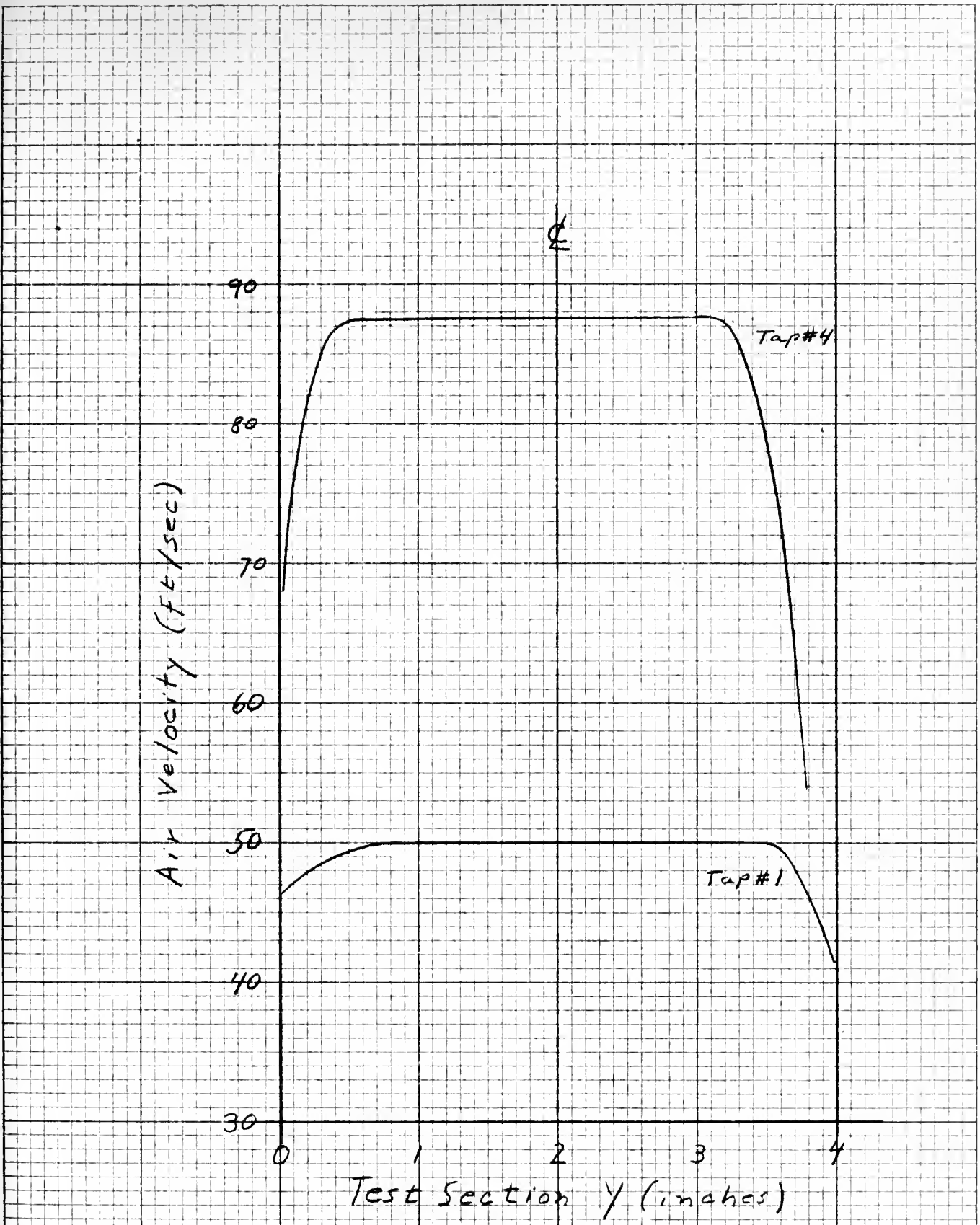

Fig. 15

Velocity Profiles for two different Tunnel Speeds

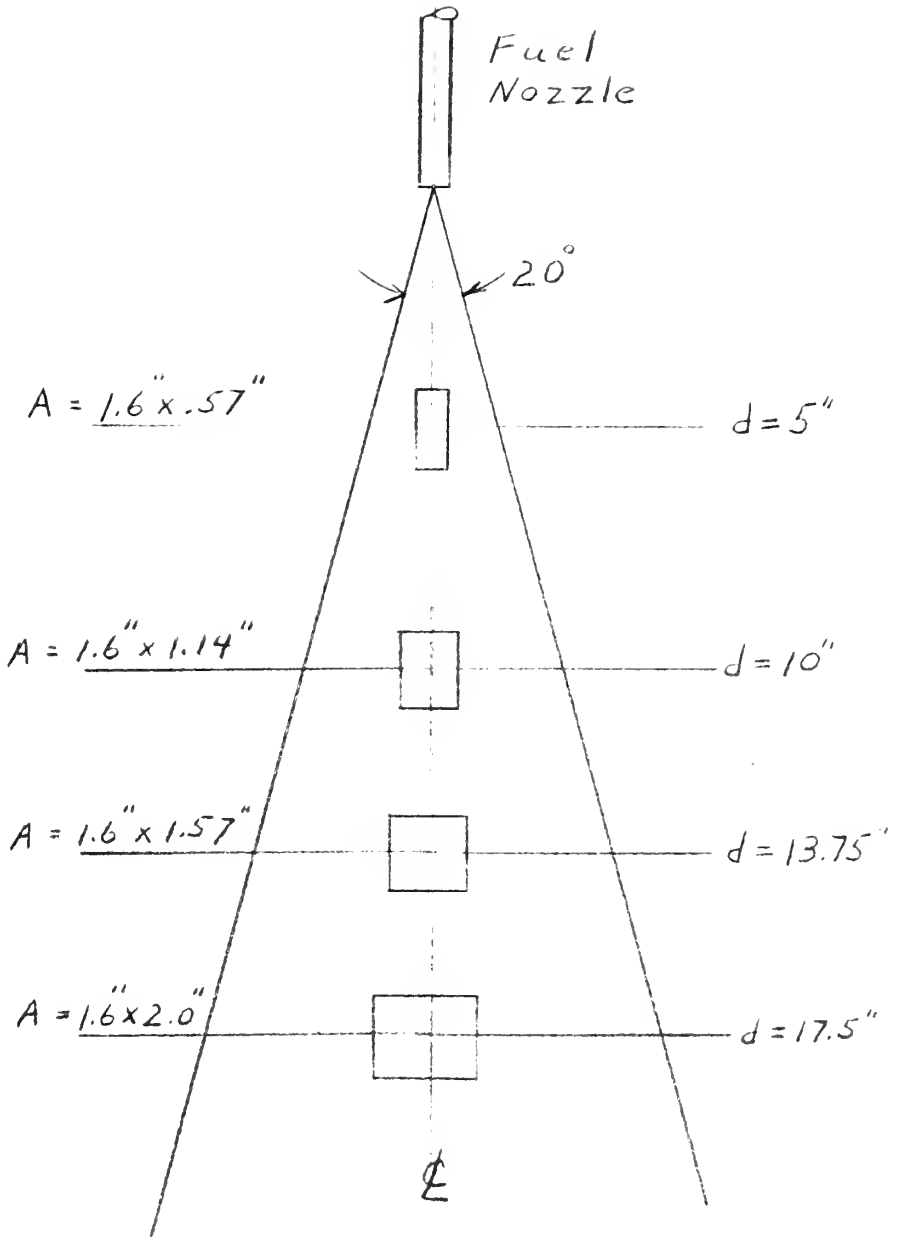

Fig. 16
Fuel Spray Geometry

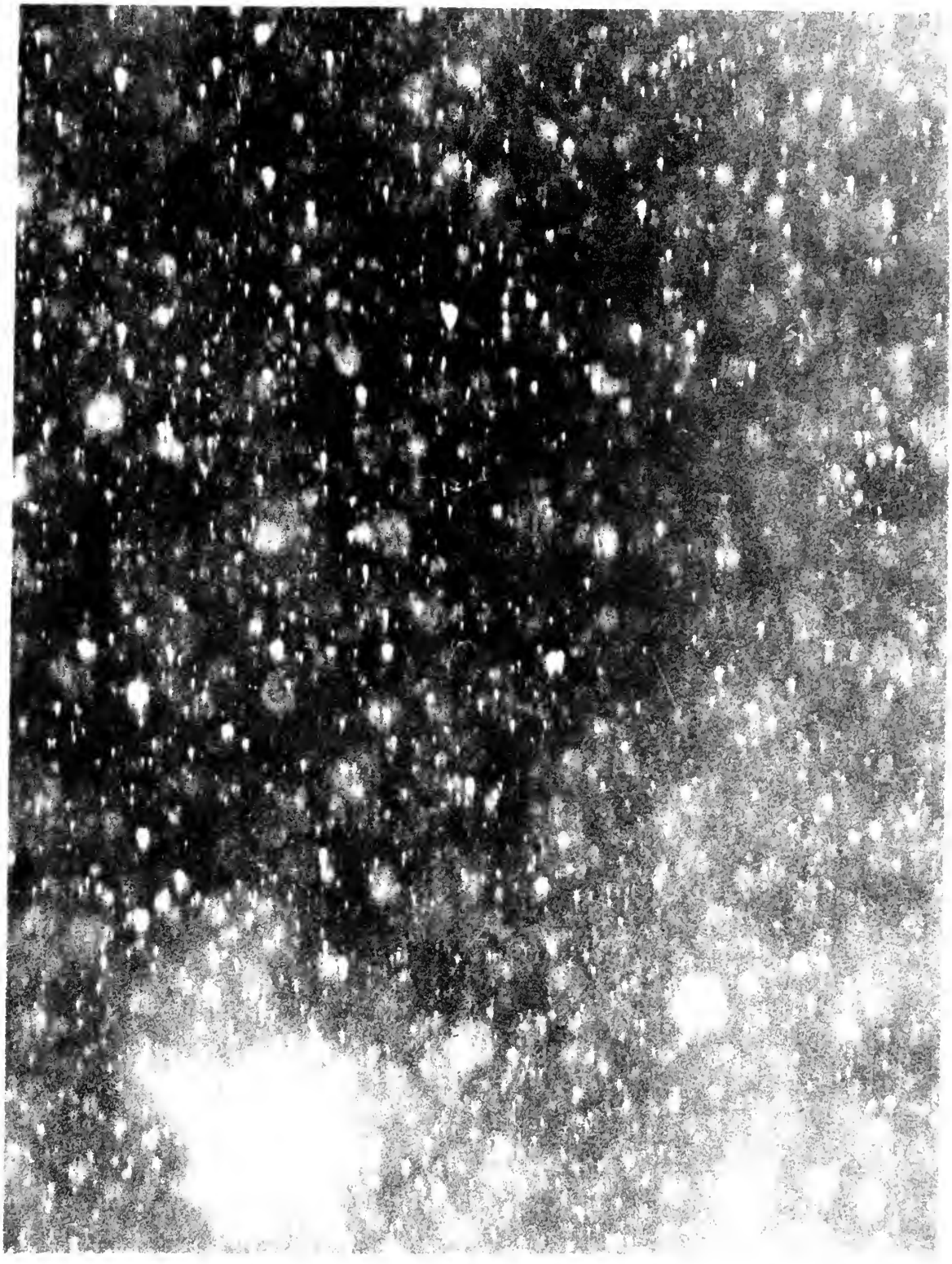

Fig. 17

Benzene [illegible]ray [illegible]Scale 1:1 .7[illegible]

Ta 150°F [illegible] a [illegible]

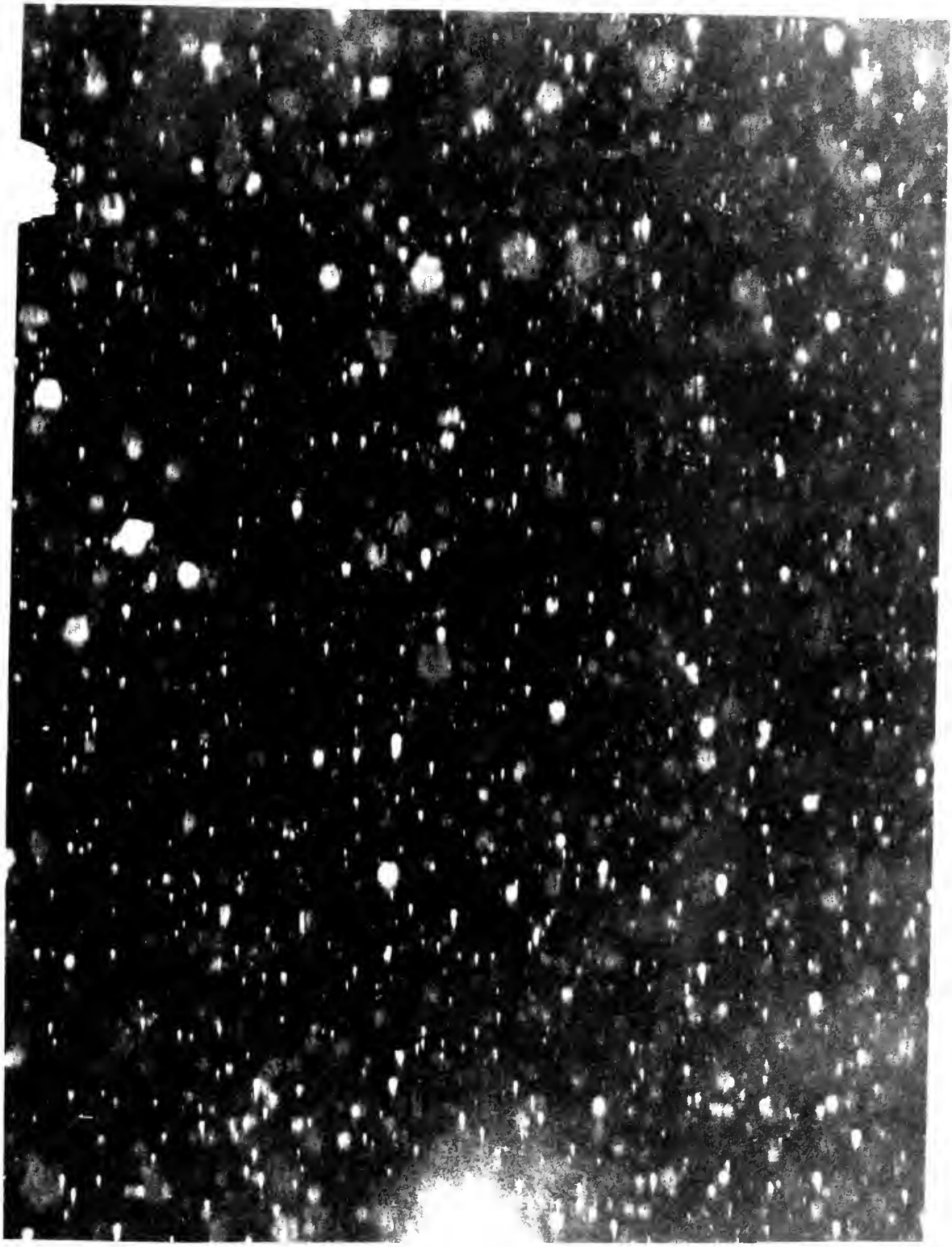

Fig. 18

Benzene Spray Scale 1:10.75

Ta 228°F d 10"

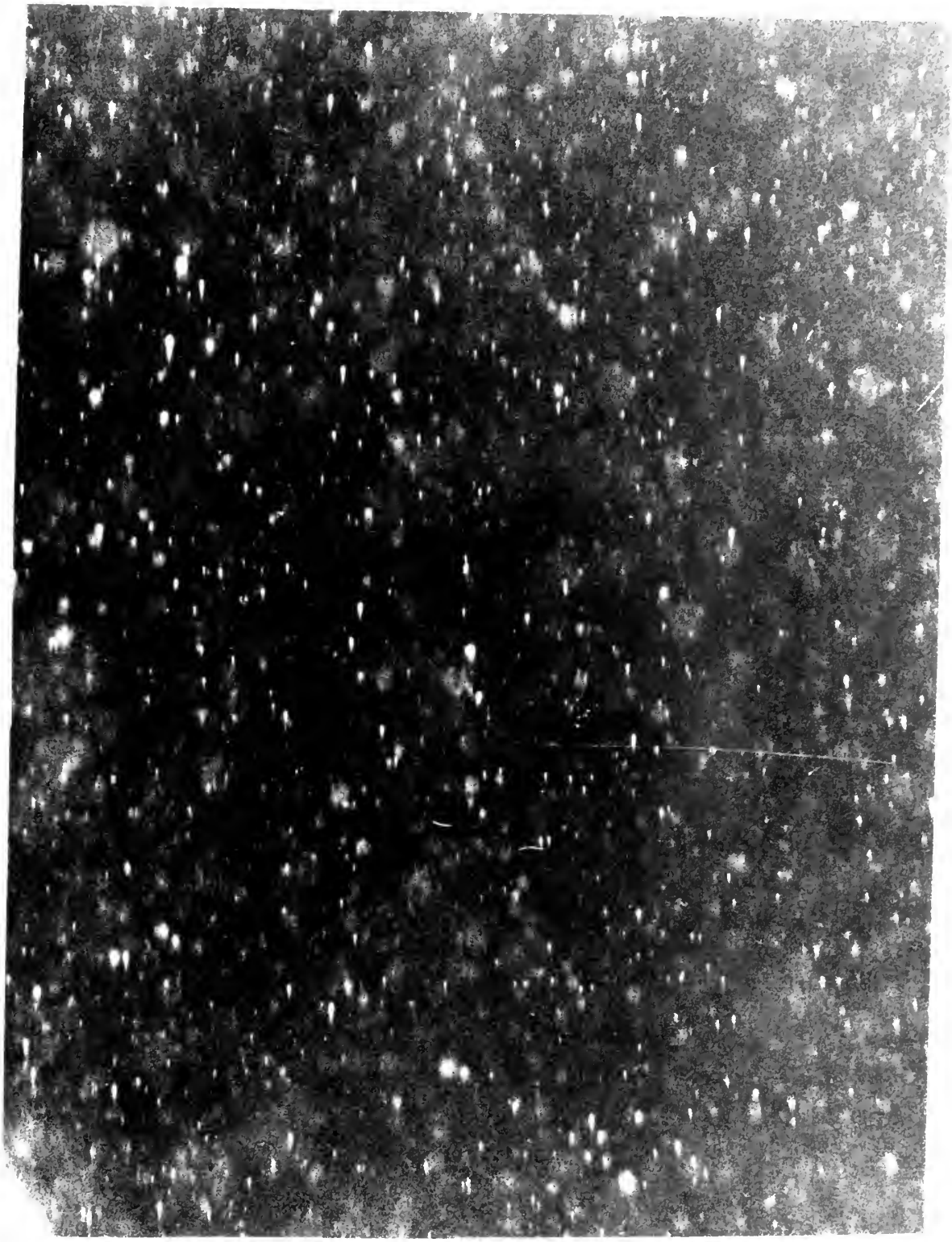

Fig. 19

Benzene spray [illegible] Scale 1:1.[illegible]

[illegible] 329°F

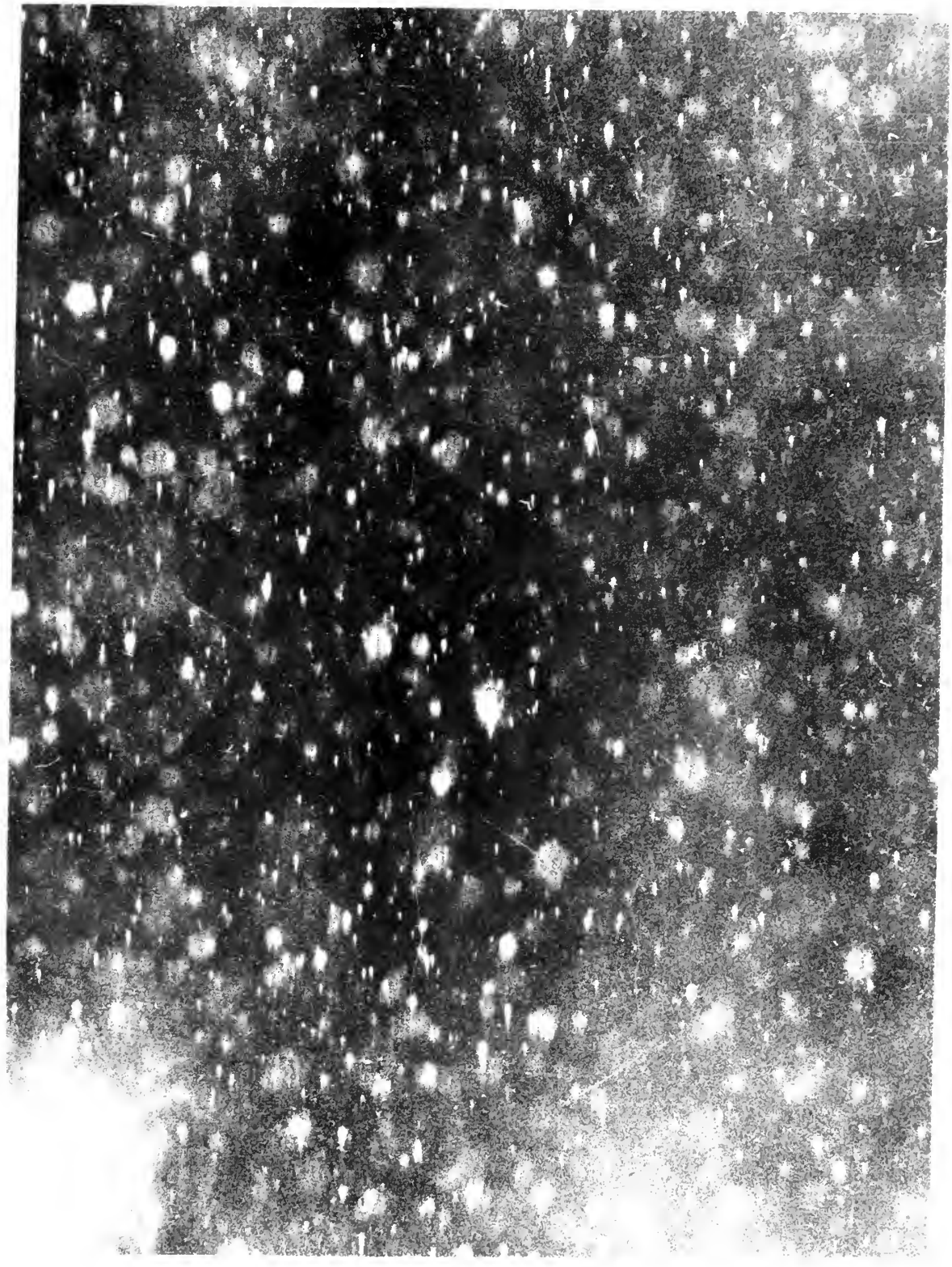

Fig. 20

Benzene Spray Scale 1:10.75

Ta 400°F d 10"

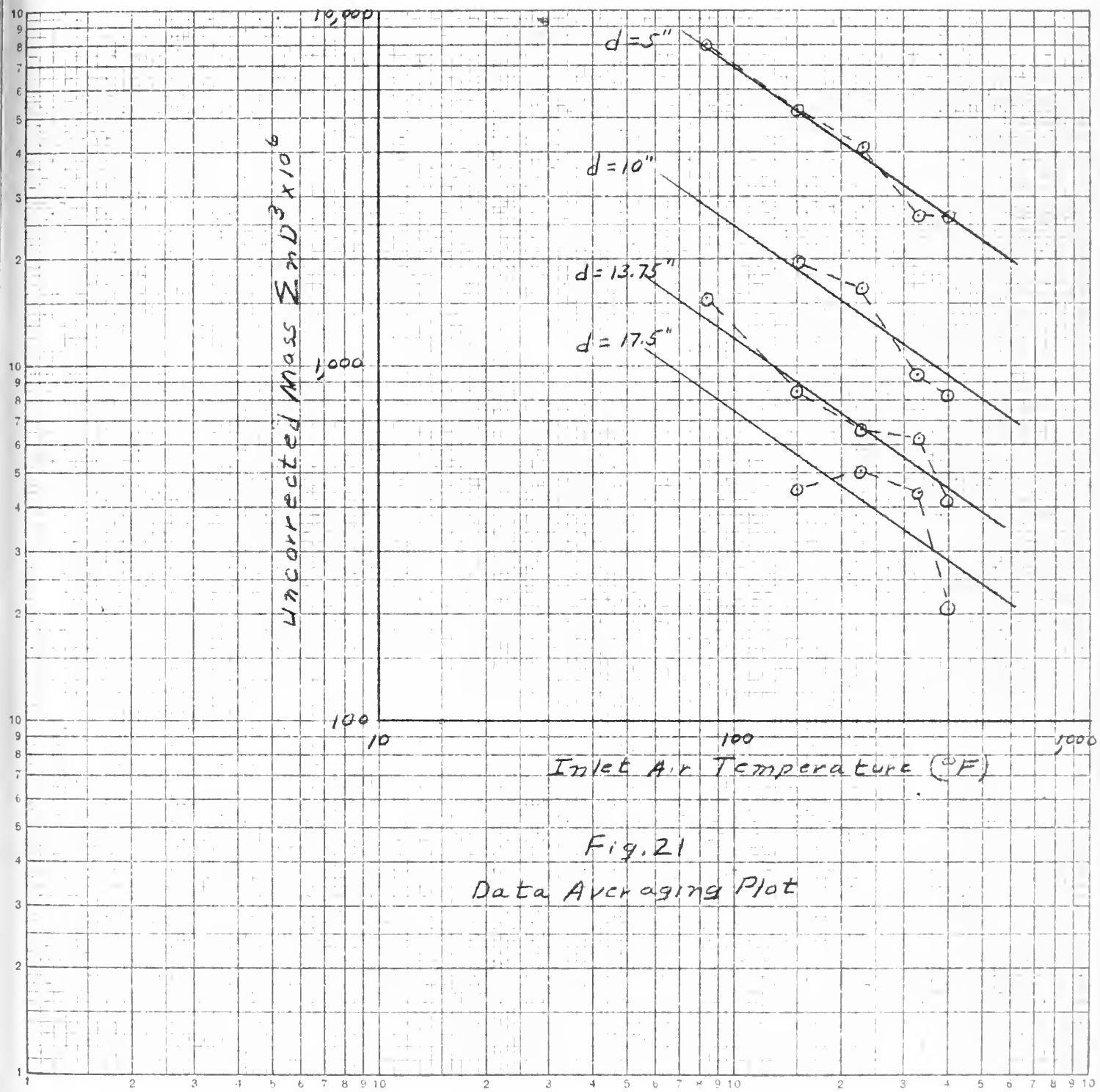

Fig. 21

Data Averaging Plot

Fig. 22

Extrapolation of $\sum nD^3$

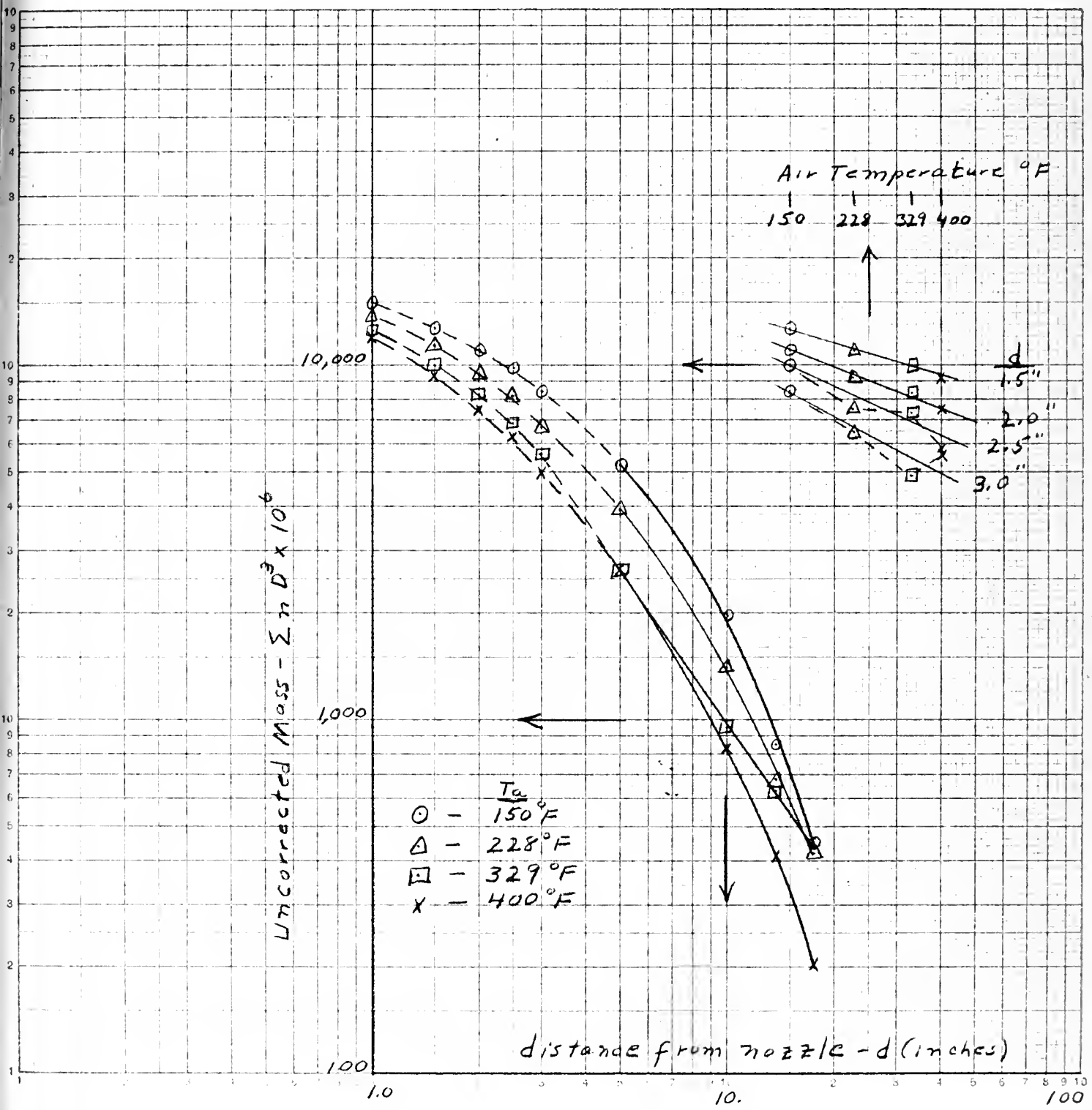

Fig. 23

Mass of Fuel Remaining

versus

Distance from Nozzle

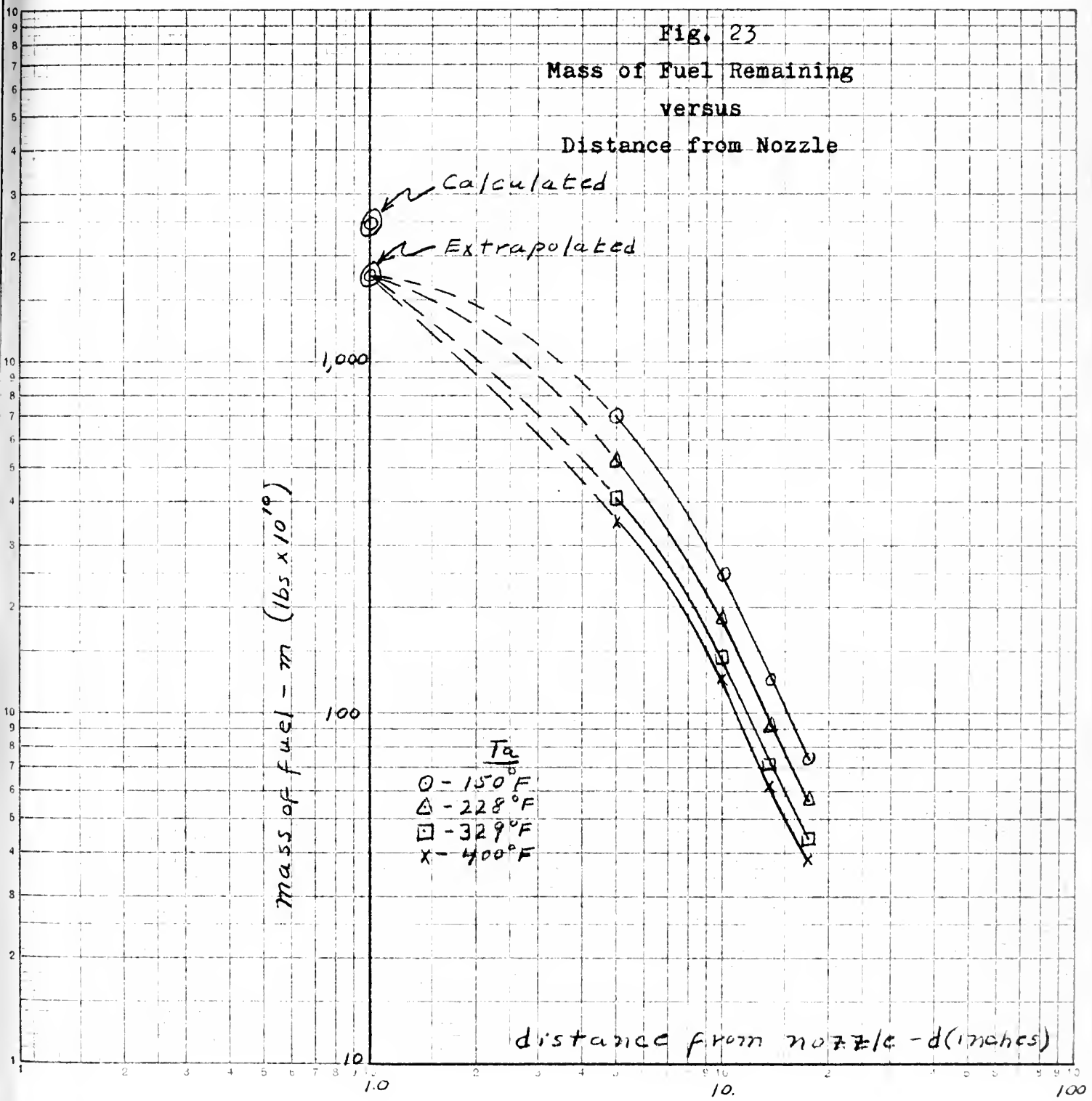

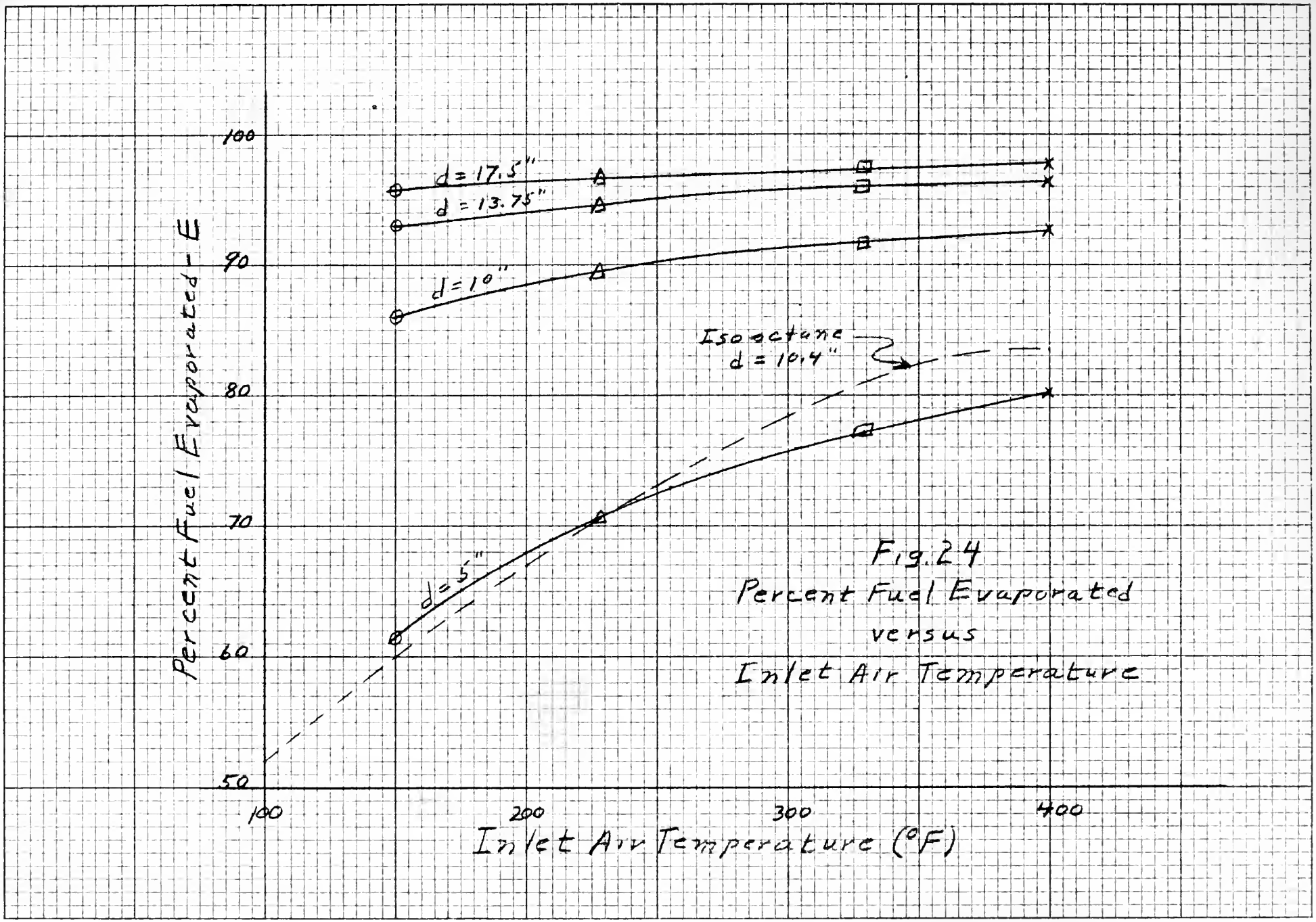

Fig. 24
Percent Fuel Evaporated
versus
Inlet Air Temperature

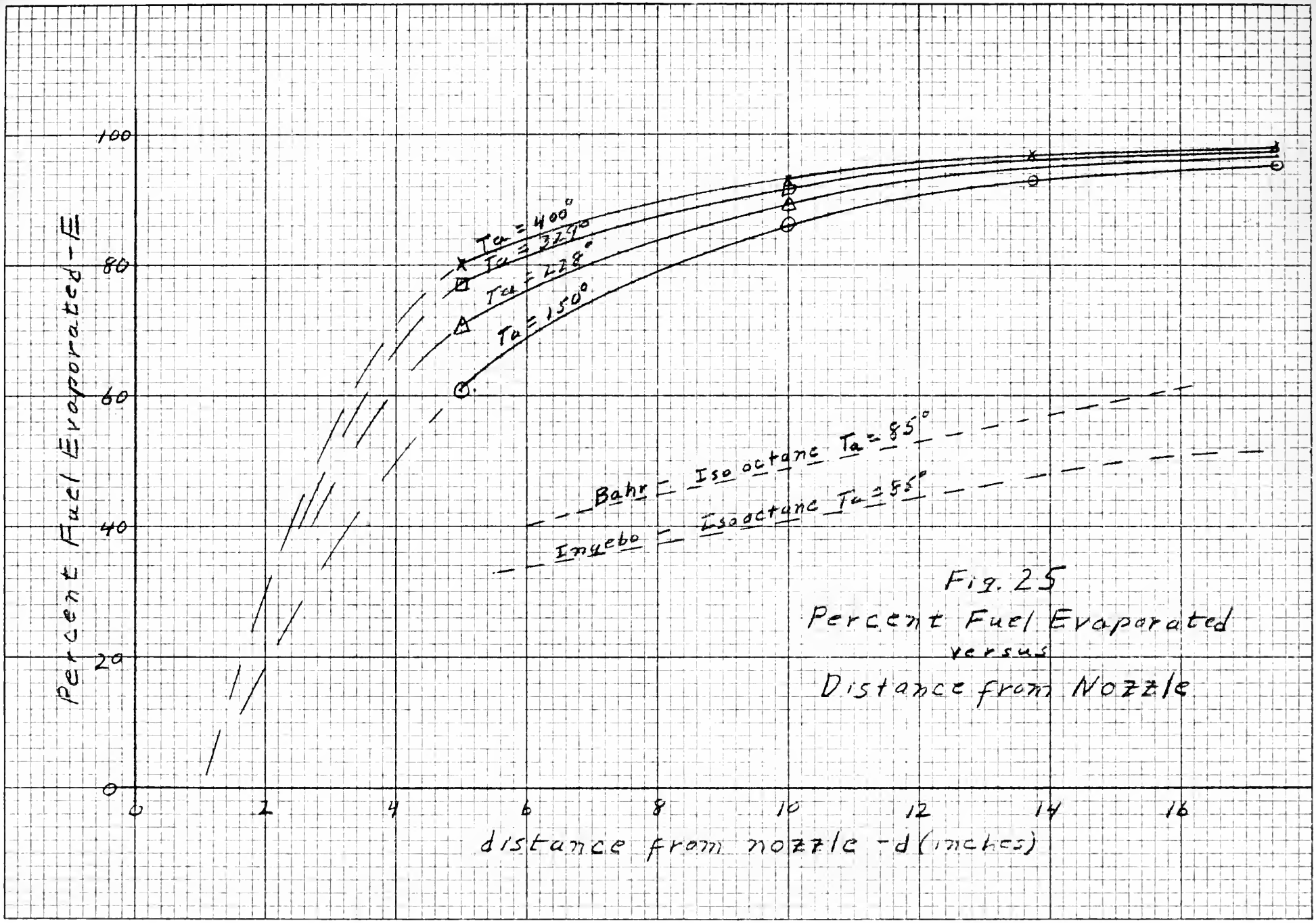

Fig. 25
Percent Fuel Evaporated
versus
Distance from Nozzle

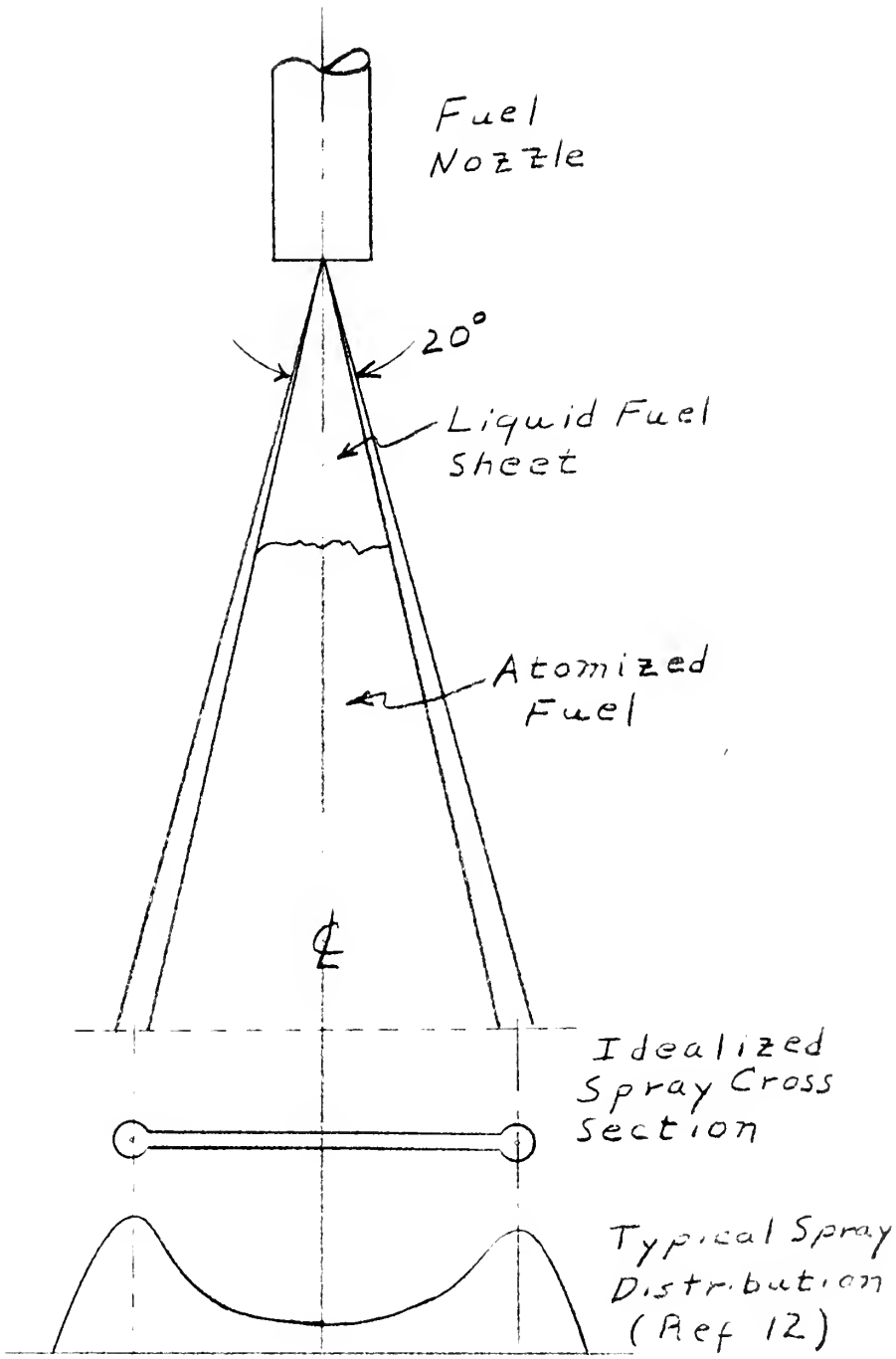

Fig. 26
Fuel Spray Distribution Pattern

Fig.27

Illustrating the concentration of fuel in edge of spray. Outlined area indicates area of drop-size count. Distance from nozzle is 5 inches.

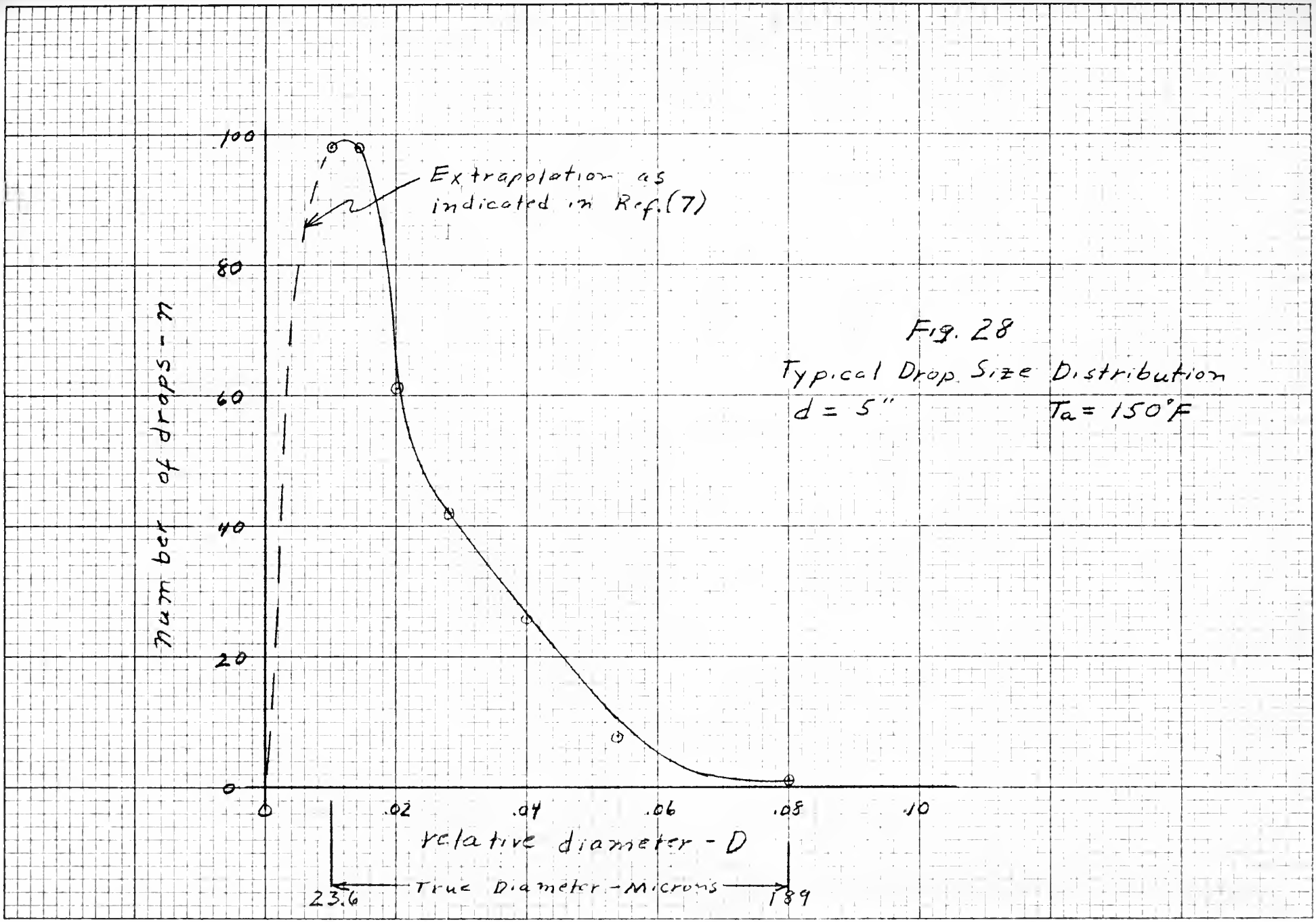

Fig. 28
Typical Drop Size Distribution
$d = 5''$ $T_a = 150°F$

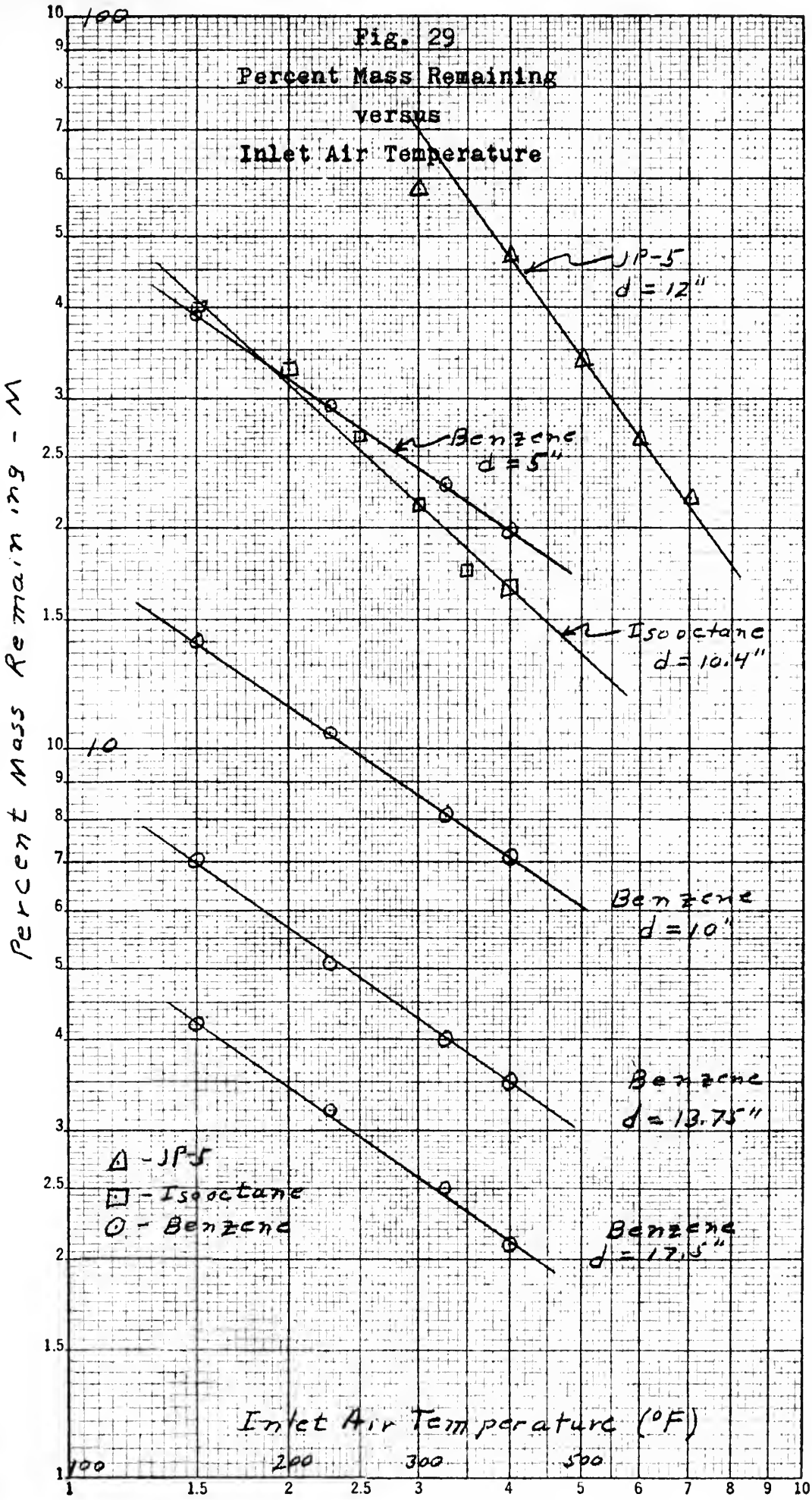
Fig. 29
Percent Mass Remaining
versus
Inlet Air Temperature
Percent Mass Remaining - %
Inlet Air Temperature (°F)
JP-5
d = 12"
Benzene
d = 5"
Isooctane
d = 10.4"
Benzene
d = 10"
Benzene
d = 13.75"
Benzene
d = 17.5"
Δ - JP-5
□ - Isooctane
⊙ - Benzene
100
200
300
500

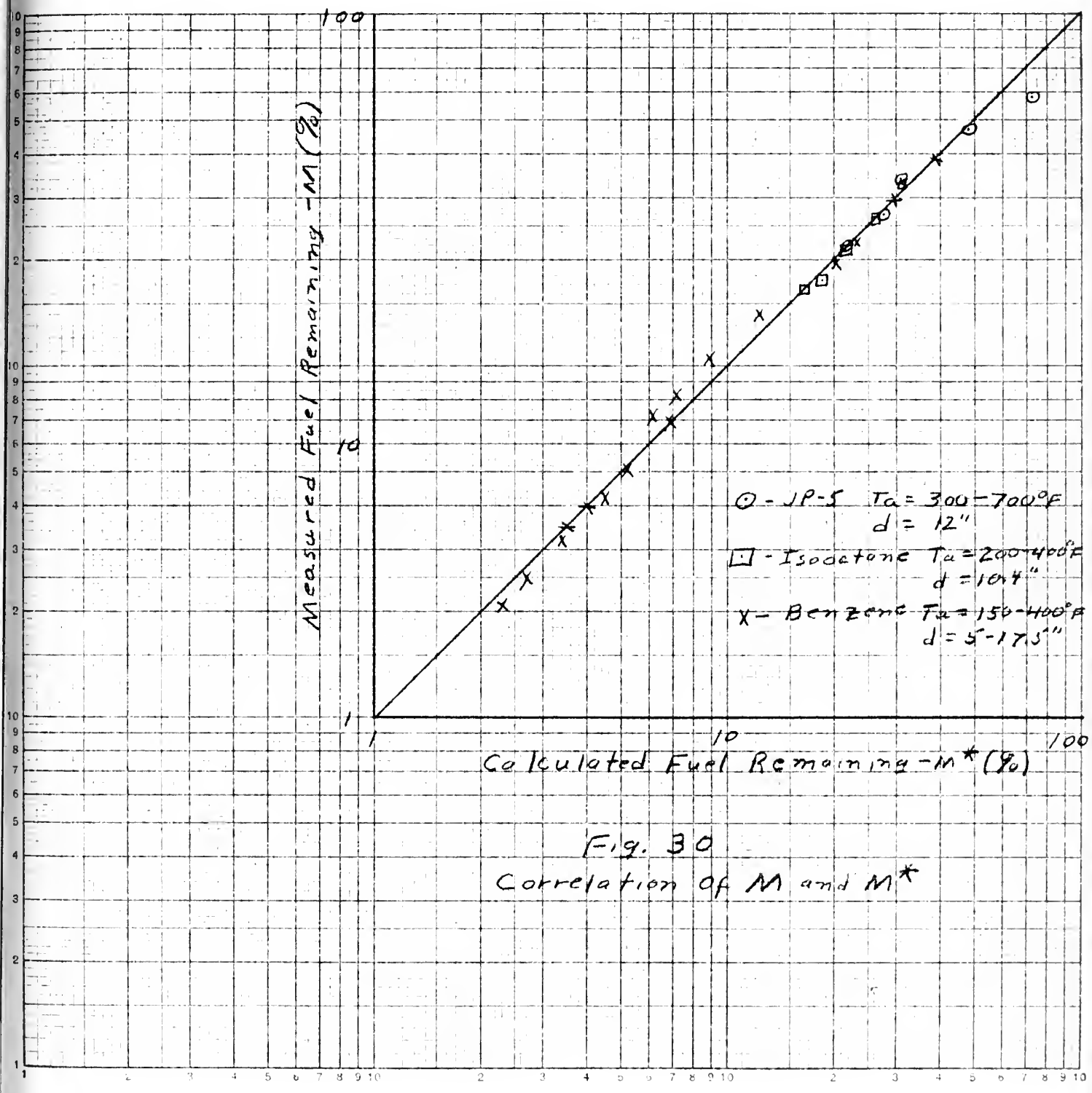

Fig. 30
Correlation of M and M*

APPENDIX A

Derivation of Empirical Formula

From a log-log plot of percent fuel remaining (M) against inlet air temperature (Ta) for the three fuels, (Fig. 29), it was noted that the slopes of the lines were roughly proportional to the boiling points of the fuels. These fuels were benzene, measured 10 inches from the nozzle; isooctane, measured 10.4 inches from the nozzle, and JP-5, measured 12 inches from the nozzle.

In order to transform the slopes into boiling points, the formula $\frac{BP}{C_1}$ = Slope was used and C_1 was found to have an average value of 257.

The three lines were then extended to intersection. Using the point-slope form of the equation of a straight line $Y-Y_o = m(X-X_o)$, or for the log-log plot, $\ln M - \ln M_1 = -m(\ln Ta - \ln Ta_1)$; M_1 was determined to be 1.1 and Ta was 6200 at intersection. The equation then took the form:

$$\frac{M^*}{1.1} = \left[\frac{Ta}{6200}\right]^{\frac{-BP}{257}}$$

M^* was then calculated from the above formula for the data temperatures of benzene, and the calculated M^* compared with the measured value of M. These two values varied by a constant factor, dependent upon

the distance from the nozzle where the data was taken.

The factor of variation, $M^*/M = f(d)$ was plotted against distance on a log-log graph. The points fell on a straight line with a slope of 1.73 and an intercept of 9.1 when $M^*/M = 1.0$. Therefore,

$$M = \frac{M^*}{\left[\frac{d}{9.1}\right]^{1.73}}$$

or,

$$\frac{M^*}{1.1} = \frac{1}{\left[\frac{Ta}{6200}\right]^{\frac{BP}{257}} \left[\frac{d}{9.1}\right]^{1.73}}$$

The variation in distance from the nozzle between the measurement of benzene, isooctane, and JP-5 still had not been accounted for. For these three fuels, the original three lines considered, the factor $\left[\frac{d}{9.1}\right]^{1.73}$ was computed, and the logarithm of this factor graphically subtracted from the original lines. The new lines, with the distance factor subtracted out, were then extended to intersection and using the point-slope form of the straight line again, the constants of the empirical equation were determined to be,

$$\frac{M^*}{1.65} = \frac{1}{\left[\frac{Ta}{3300}\right]^{\frac{BP}{257}} \left[\frac{d}{9.1}\right]^{1.73}}$$

M^* was then calculated for all available data of benzene, isooctane, and JP-5. M^* was plotted against M (the measured values) on a rectangular plot. Three

straight lines of different slopes were obtained for the three fuels. This indicated that the constant 1.65 had to be modified for each fuel. The slopes of each of these three lines was measured and multiplied by the constant 1.65. This gave the final constants for the formula as: benzene, 1.70; isooctane, 2.94; and JP-5, 4.05.

A final calculation for M^* was performed using the correlation formula in its final form. This value is plotted against the experimental measured values in Fig. 30 and indicates good correlation.

Sample Calculations

Nomograph Calculations:

From the Perfect Gas Law

$$P = \rho RT \qquad R = 24.22 \text{ in-Hg } ft^3/\text{slug } {}^\circ R$$

$$\rho = \frac{P}{RT}$$

$$\rho_a = \frac{Pa}{24.22(Ta+460)}$$

$$\rho_a = \frac{.04125\ Pa}{(Ta+460)}$$

For dynamic pressure:

$$q = \tfrac{1}{2}\ {}_a V_a^2$$

$$V_a^2 = \frac{2q}{\rho_a}$$

Specific gravity of manometer alcohol = .81

$$q = \frac{(62.4)(.81)\ h}{12} \quad \text{lbs/ft}^2$$

$$q = 4.2\ h$$

then $$V_a^2 = \frac{8.4\ h}{\rho_a}$$

Nozzle Calculations:

From Bernoulli's Equation:

$$\frac{V_{f_2}^2}{2g} = \frac{V_{f_1}^2}{2g} + \frac{P_1 - P_2}{\gamma}$$

ignoring V_{f_1};

$$V_{f_2}^2 = \frac{2g}{\gamma}(P_1 - P_2)$$

$$V_{f_2}^2 = \frac{2(32.2)(\Delta P)(144)}{54.9}$$

$$V_{f_2} = 13\sqrt{\Delta P}$$ where ΔP = fuel injection pressure drop

Since $V_{f_2} = 13\sqrt{\Delta P}$

and $P = 81.4$ p.s.i.

$$V_{f2} = 13\sqrt{81.4}$$

$$V_{f_2} = 117.5 \text{ ft/sec}$$

Conversion of $\sum nD^3_{ave.}$ to mass:

For a sphere (drop) $Vol = 4/3\,\pi r^3$ $\quad r = \frac{1}{2}D'$

$$Vol = \frac{4}{3}\pi\frac{D'}{8} = \frac{\pi}{6}D'^3 \text{ for one drop}$$

$$Vol = \frac{\pi}{6}\sum nD'^3 \text{ for all drops}$$

$D' = D/10.75$ $\quad D'^3 = D^3/1242$ scale factor

$$Vol = \frac{\pi}{6}\frac{\sum nD^3}{(1242)} \times 10^{-6}$$

$$Vol = .422\sum nD^3 \times 10^{-9} \text{ in}^3$$

$$m = Vol(\gamma)$$

$$m = \frac{.422\sum nD^3 \times 10^{-9} \times 54.9}{1728}$$

$$m = .134\sum nD^3 \times 10^{-10} \text{ lbs.}$$

Calculation of initial mass of fuel injected:

Velocity of injected fuel

$$V_{f_2} = 117.5 \text{ ft/sec} = 1410 \text{ in/sec}$$

height of photographed spray area = 9 in.

scale factor 1:10.75

tunnel distance covered by photograph

$$d = 9/10.75 = .838 \text{ in.}$$

elapsed time

$$t = .838/1410 = .594 \times 10^{-3} \text{ sec.}$$

Fuel delivery rate of nozzle

$$\dot{m}_f = .835 \text{ lb/min} = .01392 \text{ lb/sec.}$$

$$m_f = \dot{m}_f \, t$$

$$m_f = (.01392)(.594) \times 10^{-3}$$

$$m_f = 8.28 \times 10^{-6} \text{ lbs. total fuel delivered}$$

spray edge concentration allowance = 75%

$$m_f = (.25)(8.28) \times 10^{-6}$$

$$m_f = 2.07 \times 10^{-6} \text{ lbs. of uniform spray}$$

Fractional mass photographed at d = 5 in.

spray half width = 5 tan 10.5°

= 5(.185)

= .925 in.

photograph half width = $\frac{3.1}{10.75}$ = .2882 in.

$$\frac{\text{area photographed}}{\text{total area}} = \frac{A}{A_T} = \frac{.2882}{.925}$$

$$\frac{A}{A_T} = .312$$

Percent of spray in focus = 38.5%

Corrected amount of fuel delivered

$$m_i = (.312)(.385)(2.07) \times 10^{-6}$$

$$m_i = 2485 \times 10^{-10} \text{ lbs.}$$

Thesis
H357 Hawvermale 35881
An investigation of the effect
of air temperature on benzene
spray vaporization.